5-1994

Sedimentology and Foraminiferal Taphonomy in Siliciclastic Environments: The Northern Gulf of California, Mexico

Liping Zhang

Utah State University

SEDIMENTOLOGY AND FORAMINIFERAL TAPHONOMY IN SILICICLASTIC ENVIRONMENTS: THE NORTHERN GULF OF CALIFORNIA, MEXICO

by

Liping Zhang

A thesis submitted in partial fulfillment
of the requirements for the degree

of

MASTER OF SCIENCE

in

Geology

Approved:

UTAH STATE UNIVERSITY
Logan, Utah

1994

ACKNOWLEDGMENTS

I would like to express my sincere thanks and appreciation to Dr. W. David Liddell, my major professor and friend, for suggesting this thesis project, for arranging funding, and for his advice, patience, and encouragement during the period of my graduate studies. I would also like to thank Dr. Peter T. Kolesar and Dr. Robert Q. Oaks, Jr. for their careful reviewing of and pertinent comments concerning my thesis. Special thanks are extended to Dr. Ronald E. Martin, at the University of Delaware, for his kind and invaluable assistance throughout my thesis research period. Many thanks also go to Jason L. Casper, Denny J. Johnson, Mary Ann Johnson, David R. Lawrence, Daren R. Rasmussen, and David H. Stirling who spent considerable amounts of time assisting me in the field and laboratory. I would also like to express my appreciation to the other faculty and students of the Department of Geology at Utah State University for their friendship, hospitality, assistance, and support during my graduate career.

Funding for this research project was provided by National Science Foundation grant #EAR-9017968 to W. David Liddell. The School of Graduate Studies and the Provost's Office of Utah State University also provided fellowships.

Finally, I would like to give my deep thanks to my parents, Songfen Yu and Yukun Zhang, and my sister, Anping Yu, for their love, understanding, and encouragement, which made the successful completion of this project possible.

Liping Zhang

CONTENTS

LIST OF TABLES

LIST OF FIGURES

ABSTRACT

Sedimentology and Foraminiferal Taphonomy in Siliciclastic Environments: the Northern Gulf of California, Mexico

by

Liping Zhang, Master of Science

Utah State University, 1994

Major Professor: Dr. W. David Liddell
Department: Geology

Holocene sediments from intertidal and shallow subtidal zones in Bahia la Choya, Mexico exhibit significant differences based on their mineralogical content, constituent composition, textural parameters, and foraminiferal assemblages. The intertidal sediments are characterized by low calcium carbonate content, being dominated by quartz, and are moderately well sorted and coarse skewed with a fine mean grain size (M_z = 2.73 phi). Total numbers (living and dead) of benthonic Foraminifera per ml of sediment are relatively low (12/ml) in the intertidal zones. In contrast, the subtidal sediments are characterized by high calcium carbonate content, being dominated by molluscan shell fragments, and are poorly sorted and nearly symmetrically skewed with a medium mean grain size (M_z = 1.41 phi). Total numbers of benthonic Foraminifera per ml of sediment are relatively high (52/ml) in the subtidal zone.

The analysis of bioerosion intensity indicates that differences in susceptibility to bioerosion exist not only at the subordinal level but also at the generic level of Foraminifera. Overall rates of test destruction are rapid, apparently due to the combination of biological, chemical, and physical processes.

The experimental determination of test characteristics which correlate with settling or entrainment enables the delineation of foraminiferal morphotypes which are most likely to be transported. Test settling velocity is mostly affected by test size and weight. Movement threshold velocity is, also, mostly affected by test size, weight, and shape, in addition to the nature of the substrates and initial test orientation. Foraminifera from siliciclastic environments exhibit relatively low settling and movement threshold velocities. Thus, taxa from siliciclastic settings are more likely to be transported by currents than are those from carbonate environments, which show a wide range of settling and movement threshold velocities. Such information may be utilized to distinguish between autochthonous and allochthonous microfossil assemblages in the stratigraphic record.

(120 pages)

INTRODUCTION

Taphonomic analysis has been proven to be a very effective method for the reconstruction of paleoenvironments. The majority of taphonomic studies have been conducted on macroinvertebrate and vertebrate assemblages, and only a few have involved microfossils (Behrensmeyer and Kidwell, 1985). This is despite the fact that Foraminifera exhibit a tremendous variety of test compositions, microstructures, and morphologies (Tappan and Loeblich, 1988), which should result in differing susceptibilities of taxa to taphonomic alteration. Studies of Recent shallow-marine habitats and faunas result in better understanding of taphonomic processes in these environments. The variety of modern siliciclastic depositional environments in Bahia la Choya, Mexico provides an ideal place for the study of sedimentary and taphonomic processes (Fig. 1).

This research focused on two aspects: characteristics of sediments, and taphonomic alteration of Foraminifera in modern siliciclastic environments. Sedimentological characteristics (mineralogy, grain composition, and textural parameters) were determined quantitatively from sediment samples collected through a broad environmental range (inner flat, middle flat, outer flat, and subtidal zone) and from Pleistocene fossiliferous marine rocks along the margins of Bahia la Choya. These characteristics were used to interpret the

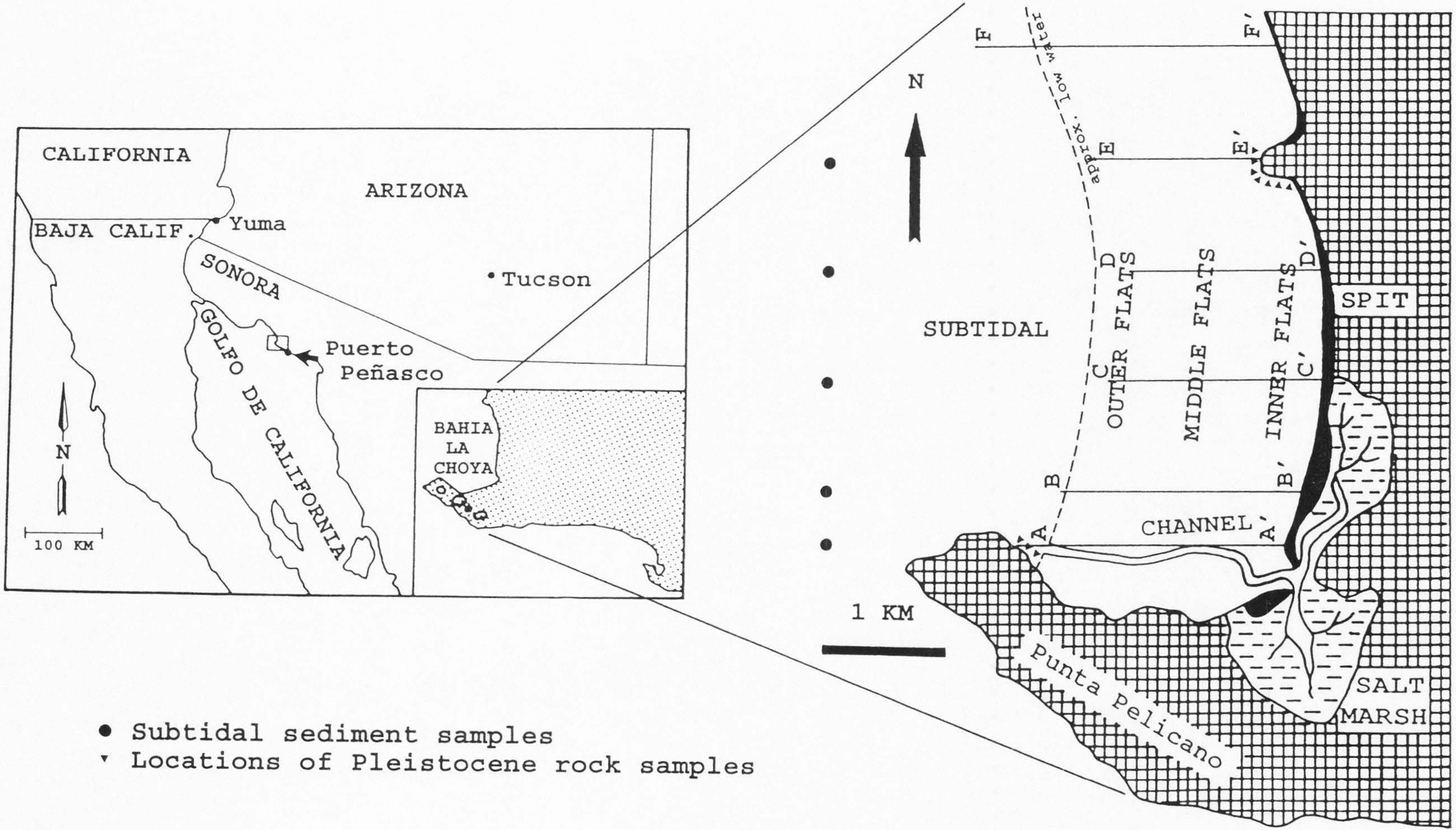

FIGURE 1-Locality map of Bahia la Choya, Mexico, showing major depositional environments and locations of six sampling traverses, labeled A-F, of this study (modified from Fürsich and Flessa, 1987; and Meldahl, 1990). The location of the distal portion of the channel is approximate.

relationships of different depositional environments in the study area. The sedimentation rate was also assessed by studies of living and dead populations of benthonic Foraminifera.

Taphonomic alteration of Foraminifera in Quaternary siliciclastic deposits was examined through analysis of bioerosion intensity and hydraulic properties of tests. The study has identified taphonomic characteristics of test morphotypes which should be applicable to different environments and time intervals.

Previous Work

Studies of modern siliciclastic sedimentation and taphonomy in the northern Gulf of California have primarily been restricted to Puerto Peñasco and adjacent areas such as Bahia la Choya and Estero Marua (Sandusky, 1969; Flessa and Ekdale, 1987; Fürsich and Flessa, 1987; Meldahl, 1987a,b; Sumpter, 1987; Meldahl, 1990).

Detailed studies on the distribution of living benthonic Foraminifera have been accomplished in Todos Santos Bay of Baja California, Mexico by Walton (1955), in the northern Gulf of Mexico by Phleger (1960), and in the northern Gulf of California by Sandusky (1969).

Studies on bioerosion of macroinvertebrates have been conducted in the northern Gulf of California by Stearley and Ekdale (1989). Studies on bioerosion of Foraminifera have been done at the island of Curacao (Netherlands Antilles) by Kloos (1982), in the Bahamas by Peebles and Lewis (1988), and at San Juan Island (Washington, USA) by Shroba (1993). Additional studies of bioerosion by microbial endoliths have been reported by Golubic et al. (1984) and Silva de Echols (1993).

Studies of the hydraulic properties of Foraminifera have been done by Maiklem (1968); Berger and Piper (1972); Warg (1973); Kontrovitz et al. (1978, 1979); Fok-Pun and Komar (1983); Cunningham et al. (1989); Liddell et al. (1990); Martin and Liddell (1991); and Oehmig (1993).

In addition, considerable work on foraminiferal biofacies and sedimentary environments in Pleistocene and Holocene deposits along the north coast of Jamaica has been done by Boss and Liddell (1987a,b); Liddell et al. (1987); and Martin and Liddell (1988, 1989). Studies of taphofacies represented by foraminiferal assemblages have also been conducted at Discovery Bay, Jamaica (Cunningham et al., 1989; Kotler et al., 1989; Liddell and Martin, 1989; Liddell et al., 1990; Martin and Liddell, 1990).

Location of Study

The principal study area, Bahia la Choya, is a shallow embayment located along the northeastern Gulf of California, 15 km northwest of Puerto Peñasco, Sonora, Mexico (Fig. 1). Puerto Peñasco, at 113°33′ W longitude and 31°18′ N latitude, is situated in the Sonoran Desert 106 km south-southwest of

Lukeville, Arizona and reached by Mexican Highway 8. Average surface-water temperatures range from 30-32°C in the summer to 10-14°C in the winter (Flessa and Ekdale, 1987). The range of salinities is 35-36‰ in offshore surface waters and 36-39‰ in shallow coastal waters (Flessa and Ekdale, 1987). Tides in the northern Gulf of California are of very high range and of the mixed and semidiurnal type, which generates a broad intertidal zonation and high current velocities. The spring tides can commonly reach 8 or 9 meters in amplitude during new- and full-moon phases (Flessa and Ekdale, 1987; Fürsich and Flessa, 1987). A variety of modern depositional environments, including beach; inner, middle, and outer tidal flats; tidal channel; salt marsh; and the offshore subtidal area are present in the study area (Fig. 1).

METHODS

Field Methods

A total of 250 bulk sediment samples was collected along six parallel traverses across bathymetric gradients on the tidal flats at Bahia la Choya in July 1991, January 1992, and July 1992. An additional eight bulk sediment samples were collected from the shallow subtidal areas along continuations of the first five traverses during July 1991 and July 1992 (Fig. 1). The lengths of these traverses vary from 1400 m to 2500 m. The distance between samples in each traverse is between 100 and 130 m (above the subtidal zone). The six traverses were designed to encompass all accessible environments present at Bahia la Choya such as subtidal, intertidal flats, tidal channel, salt marsh, and beach (Fig. 1). In order to maximize accessibility, sampling was accomplished during the new- and full-moon phases as determined by the tide calendar for the northern Gulf of California (Thomson, 1991-1992).

At each sample site on the tidal flat, a shovel was used to collect the upper 40 cm of sediment. Subtidal bulk-sediment samples were collected by surface grab via scuba diving. Approximately 500 gm of sediment were included in each sample, and two samples were taken at each site. One of the sample replicates was fixed immediately after collection in the field by a solution of formaldehyde with calcium carbonate as a buffer to preserve foraminiferal protoplasm and tests during the time period between the date of collection and final processing. In addition to the bulk-sediment samples, 37 samples of shells, rubble, and macrophytes were collected in the field and immediately fixed with formaldehyde. The other sediment samples were treated following collection by drying in an oven at approximately 80°C.

Pleistocene fossiliferous marine rock samples were collected from outcrops on the northeastern and southwestern margins of Bahia la Choya (Fig. 1). At each designated site, at least one rock sample was taken vertically from the top, middle, and bottom of the outcrop for constituent-particle analysis (Fig. 2). The weight of each rock sample was approximately 800 gm.

Laboratory Methods

The dry sediment samples were subdivided into portions for insoluble-residue, constituent-particle, and grain-size analysis by use of a mechanical splitter. Each subsample consisted of approximately 50 to 260 gm.

Insoluble-Residue Analysis

Fifty-nine sediment samples from six traverses were used for this analysis. Approximately 50 gm of each sample were placed in preweighed glass containers. The carbonate material was dissolved with 20% hydrochloric acid. A concen-

FIGURE 2-Pleistocene outcrop showing locations of rock samples which were taken from the top (T), middle (M), and bottom (B) of the outcrop. Height of outcrop is approximately 2 m.

tration of 20% was chosen to avoid loss of insoluble material due to frothing over the top of the containers, which occurs when more concentrated hydrochloric acid is used (Ireland, 1971). New acid was added every 12 hours until carbonate digestion was complete. The solution above the insoluble residue was then siphoned off and passed through a Buchner funnel with a preweighed Whatman No. 40 ashless filter paper inside. Following the dissolution of carbonate material, the insoluble residues in the container were rinsed with distilled water three times to remove spent and excess acid. After each rinsing the contents were settled for 12 hours and then the supernatant was again siphoned off and passed through the filter paper. The insoluble residues in the container and on the filter paper were dried in air for 72 hours to avoid any physical change and possible weight loss by the sample due to use of a oven. A test of different time intervals for drying samples was performed. The results showed that 72 hours were optimum for drying samples in air without further weight change and waste of time. The insoluble residues were then weighed with an OHAUS Model B 1500 D electronic balance having a precision of 0.007 gm to determine the weight ratios of noncarbonate constituents and carbonate constituents to the whole sample.

Further separation of the organic insoluble residue from the inorganic insoluble residue in each sample was made by baking the residues in evaporating dishes in an oven at 450°C for 8 hours. The baking time was chosen according to a test which showed that 8 hours were adequate to fully break down the organic components of the insoluble residue. The sample of remaining inorganic insoluble residue was cooled in a desiccator and weighed to determine the weight ratios of the inorganic insoluble residue and the organic insoluble residue to the whole sample.

Constituent-Particle Analysis

In order to bind unconsolidated sediments for thin-sectioning, a casting resin was used to impregnate 12 sediment samples. Interstitial air within sediments was drawn out by using a vacuum pump. After the samples were impregnated and hardened, thin sections were made by standard procedures.

An Olympus BH-2 Polarizing Microscope with a mechanical stage that has graduations along both axes was used for quantitative constituent-particle analysis of the thin sections. The point counting was done by counting individual grains at the intersection of the crosshairs at equidistantly spaced points along equally separated linear traverses across the slide. The number of points to be counted for each slide was determined by rarefaction (Sanders, 1968), which indicated that counting 300 - 400 points was sufficient to describe most sediment sample in this study (Fig. 3).

Ten poorly cemented Pleistocene rock samples were uti-

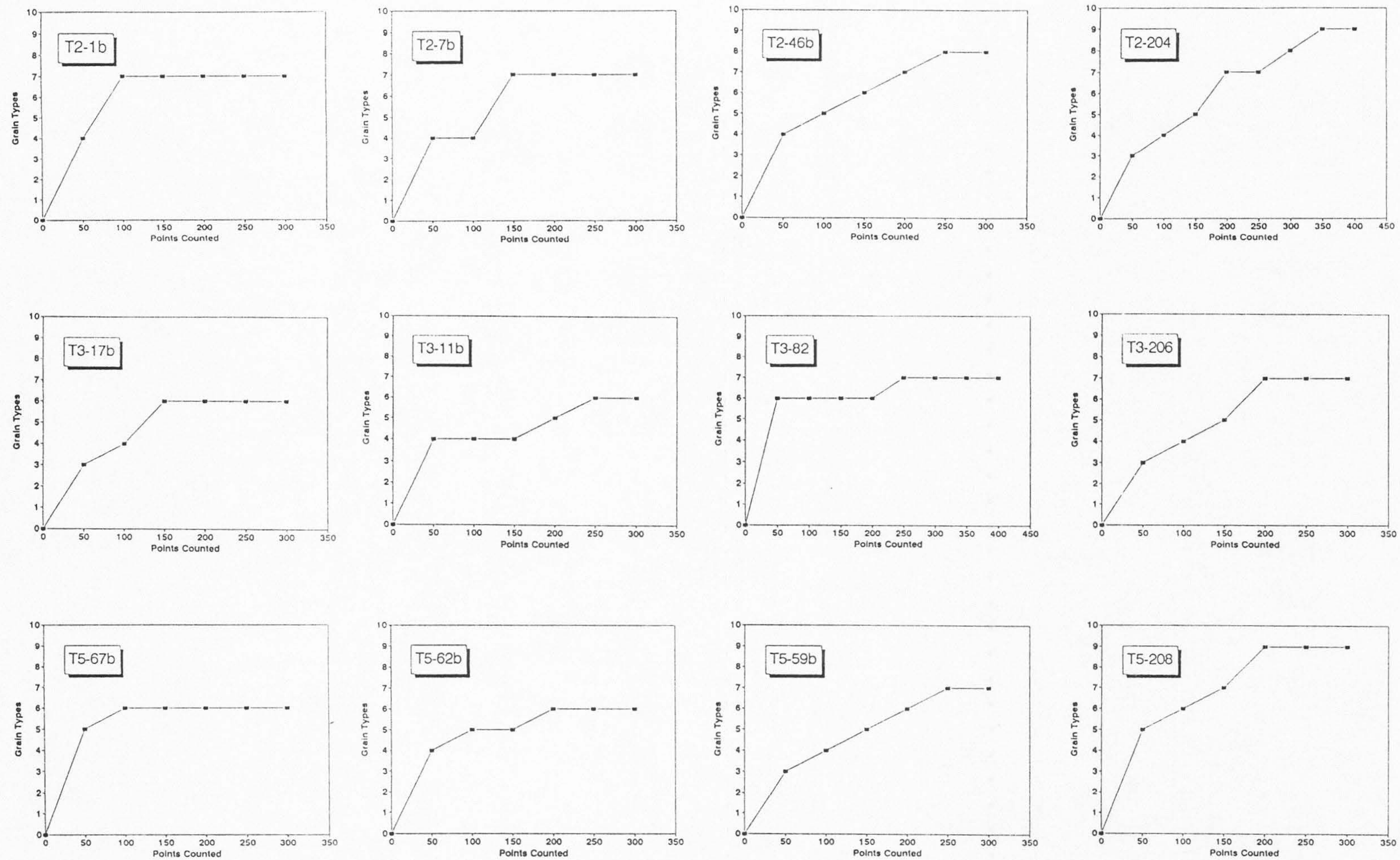

FIGURE 3-Rarefaction curves for thin-section point-counts of sediment samples (T2 = Traverse B-B', T3 = Traverse C-C', T5 = Traverse E-E'; Fig. 1).

lized for constituent-particle analysis (Fig. 4) and were prepared by the same method of impregnation used for unconsolidated sediment sectioning. The rarefaction analysis of thin sections of Pleistocene samples also indicated that counting 300 - 400 points was sufficient to describe each rock sample (Fig. 5).

Grain-Size Analysis

The size distribution of 42 sediment samples was determined by sieve analysis. Approximately 100 to 260 gm of sediment per sample were used for sieving. A nest of standard sieves from -2 to +4 phi, at quarter phi intervals, was built up, with successively coarser sieves upward. Half-height sieves were used because of the large number of sieves employed. The sieve set was then placed in a Syntron Test Sieve Shaker and shaken at a setting of 80 volts for 15 minutes. Ingram (1971) recommended 15 minutes of shaking as optional for effectively sieving the sediment without significant single-particle breakage (no further distribution change in grain size). The weight of each fraction was recorded to 0.01 gm with an OHAUS Model B 1500 D electronic balance. Two manipulations were employed to interpret data from the sieve analysis: (a) plotting data as histograms and cumulative frequency curves; (b) computation of descriptive statistical textural parameters (median, mean, standard deviation, and skewness) from intercepts taken visually from

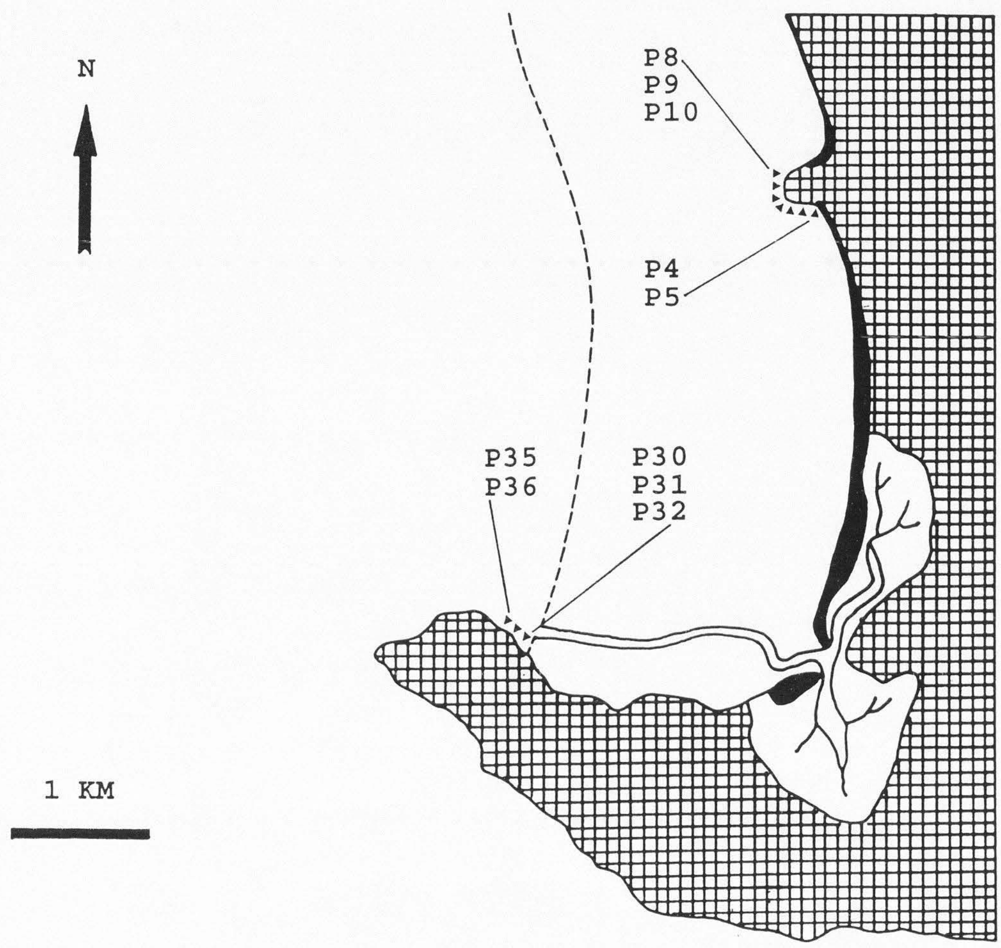

FIGURE 4-Locations of Pleistocene rock samples from Bahia la Choya, Mexico (modified from Meldahl, 1990).

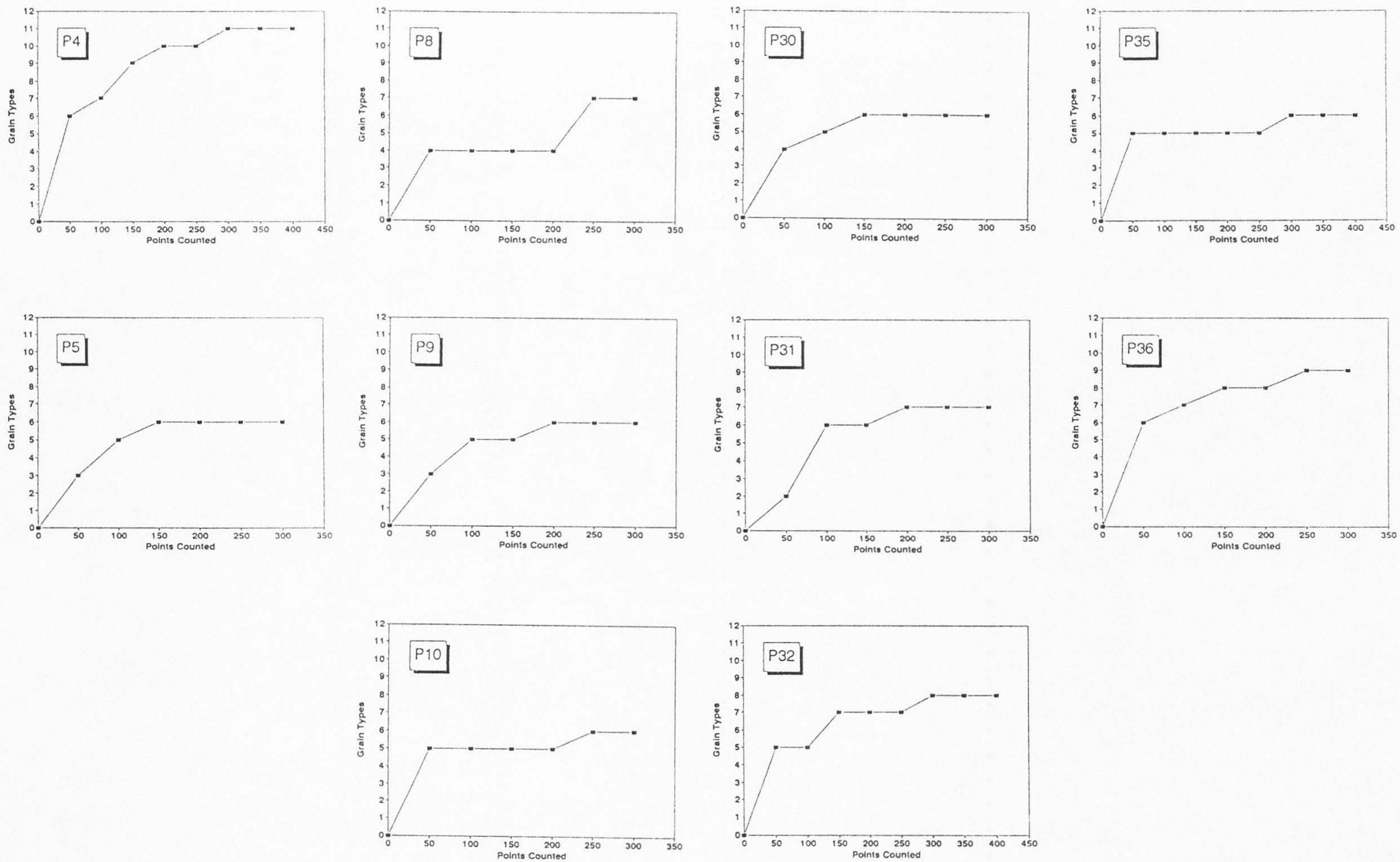

FIGURE 5-Rarefaction curves for thin-section point-counts of Pleistocene rock samples (refer to Figs. 2 and 4).

cumulative frequency curves (Folk, 1968).

Distribution Studies of Living and Dead Benthonic Foraminifera

In order to differentiate the living and dead populations of benthonic Foraminifera in the study area, the sediment, shell, rubble, and macrophyte samples fixed with formaldehyde were processed with heated saturated Sudan Black B solution. According to the staining technique described by Walker et al. (1974), a saturated solution was first prepared by dissolving 10 gm of Sudan Black B in one liter of 70% ethanol. The 250 gm samples were washed with distilled water through a bank of two sieves, 2 mm and 0.063 mm, to remove any sea water, fixative, very coarse sediments, very fine sediments, and organic debris. Next, the washed samples were placed in glass containers, in which a sufficient amount of the heated (40°C) saturated solution of Sudan Black B was added to completely immerse the samples, and stirred thoroughly to mix. The containers and samples were then transferred to a water bath regulated to 40°C for the duration of the 30-minute staining period. After staining, the excess stain was decanted and the samples were washed with 70% ethanol and distilled water through a sieve (0.063 mm) to remove the excess stain from all specimens of dead Foraminifera. Finally, samples were allowed to air dry.

In order to separate Foraminifera from sediments, a density-separation technique involving a carbon-tetrachloride solution was used (Brasier, 1980). Prior to processing, a test was done which demonstrated that the carbon-tetrachloride solution did not dissolve the Sudan Black B stain from foraminiferal tests. Approximately 40 ml of each sample were placed in a glass beaker containing a sufficient amount of carbon-tetrachloride solution to completely immerse the sample. Samples and the carbon-tetrachloride solution were then stirred vigorously with a glass rod, resulting in flotation of the relatively lighter Foraminifera while the heavier quartzose sediments sank to the bottom of the beaker. The solution with floated Foraminifera on the surface was then decanted onto a paper towel that was inserted into a funnel placed in a collecting vessel. Foraminifera on the paper towel were dried in air, and were picked under a WILD M5A stereomicroscope with a small artist's brush (size 0). The stained tests (alive at the time of sampling) and nonstained tests (dead at the time of sampling) were identified and counted separately. The number of Foraminifera per ml were determined based on the "volume-method" theory (Walton, 1955; Phleger, 1960). In order to examine the relationship between the living and total populations of benthonic Foraminifera, a ratio of "L/T" was calculated as follows:

$$R = \frac{\text{living population}}{\text{total population}} \times 100$$

where the total population is the sum of living and dead populations.

Bioerosion-Intensity Analysis

In order to determine the degree of bioerosion occurring in the study area, two methods were used. First, eleven specimens each of *Quinqueloculina seminulum* (suborder Miliolina) and ten specimens of *Elphidium articulatum* var. *rugulosum*, *Elphidium* cf. *E. crispum*, and *Elphidium* cf. *E. gunteri* (suborder Rotaliina) were randomly picked from surface sediment samples from inner and outer intertidal, and shallow subtidal zones at Puerto Peñasco so that any change in bioerosion intensity of the tests could be examined. All specimens were photographed with a Hitachi S-4000 Scanning Electron Microscope with Link Analytical XL equipment and Kodak T-MAX 100 professional film at 100x (field of view encompassing entire test). From these enlarged photos, the ratio of the surface area damaged by bioerosion to the surface area of the whole test was determined by digitizing photographs using MIPS (Map and Image Processing System by MicroImages).

Second, 10 lengths of polyvinyl chloride (PVC) pipe, each bearing well-preserved Foraminifera, were employed to test bioerosion intensity against Foraminifera in the field. Pipes to which intact Foraminifera were epoxied were divided into 10-cm increments above the sediment-water interface and

5-cm increments below the sediment-water interface, and ending 2.5 cm from the top end and 15 cm from the bottom end (Fig. 6). At each mark, three flat cuts, 1 cm wide by 2 cm high, were ground 2-3 mm deep into the pipe. The cuts protected the Foraminifera from damage during insertion and removal of pipes. Each pipe, thus, possessed four stations (+20 cm, +10 cm, sediment-water interface or 0 cm, and -5 cm) and each station had three cuts, all at 90° orientation to each other (Fig. 6). In each cut, at least three specimens of each selected species were epoxied for a total of three to six specimens of each for every station on every pipe. Each pipe had, thus, at least 12 specimens of each species employed. In addition to Mexican species of Foraminifera, Jamaican species from carbonate environments were used for comparison in this study. Narrow (approximately arm diameter) holes were excavated by hand and the pipes were buried in them at the designated sites of the study area (Fig. 7). Pipes were carefully excavated and retrieved from the field after 6 months.

Transport Analysis

In order to better understand taphonomic alteration of foraminiferal assemblages in different environments, test transport potential was analyzed by settling-tube and flume experiments. Specimens of five of the most common species in the study area were carefully selected to minimize the ef-

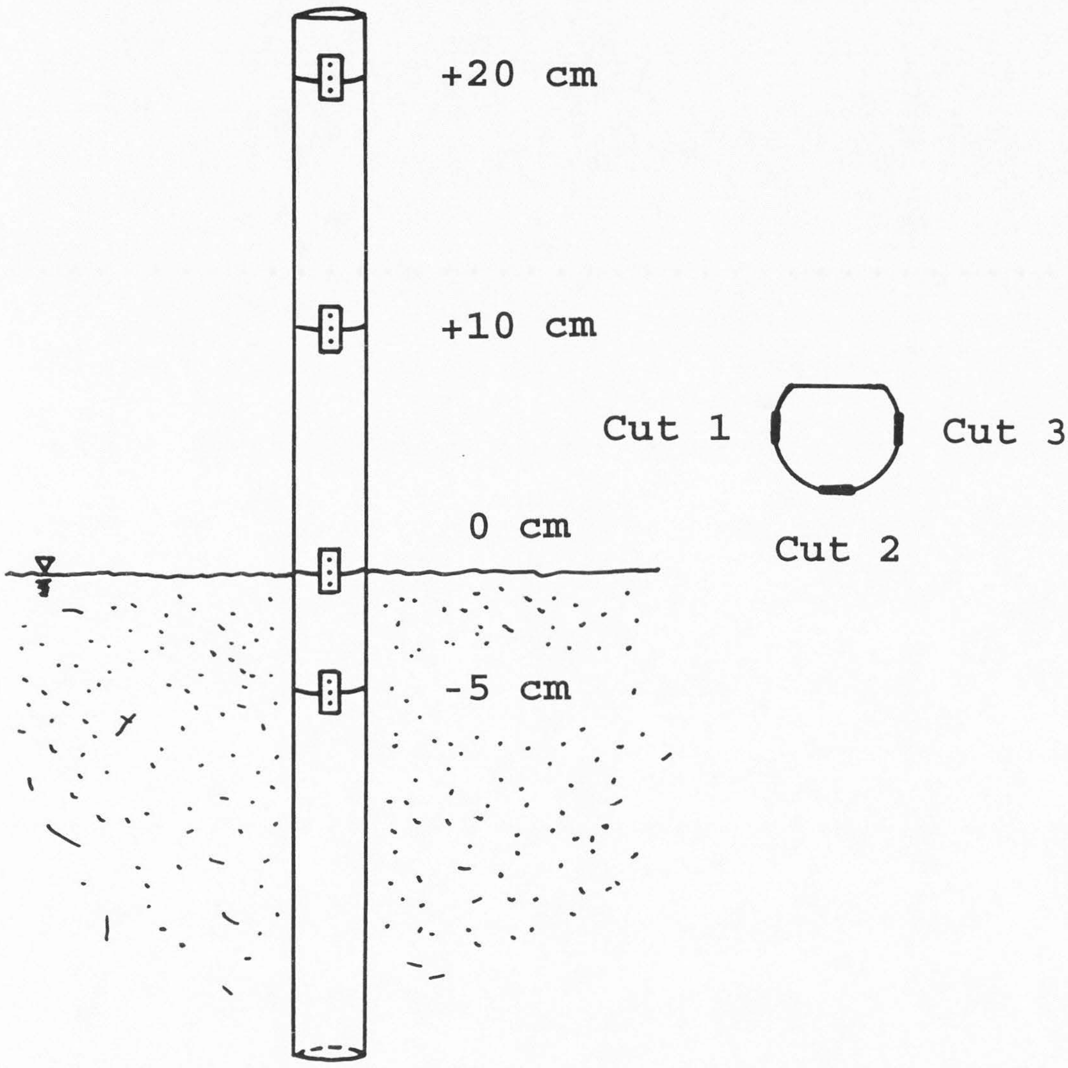

FIGURE 6-Positions of specimens along PVC pipe used in field study of foraminiferal bioerosion.

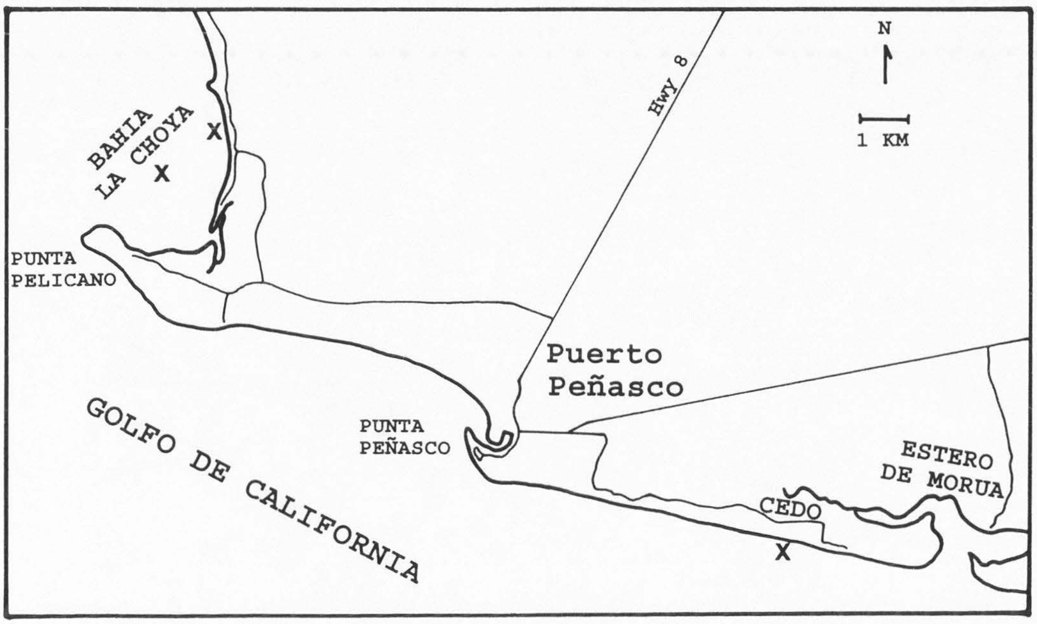

FIGURE 7-Locations of the bioerosion experiments (indicated by "X"; modified from Flessa and Ekdale, 1987).

fects of prior solution and abrasion of the tests. Prior to the hydraulic experiments, each specimen was measured by a binocular microscope with an ocular micrometer. Dimensions were recorded in millimeters to ± 0.01 mm. Three dimensions were measured for each specimen, the longest intercept (D_l), the shortest intercept (D_s), and the intermediate intercept (D_i), all at approximately 90° orientation to each other (orthogonal)(Fig. 8). All specimens were dried to constant weight in 5-ml polystyrene weighing boats for 24 hours in air. Then, weighing was performed with a Cahn C-31 Microbalance to a precision of 0.0001 mg. The dimensions and weights obtained were used to calculate or estimate the various test parameters shown in Table 1. Because of the irregular shapes of foraminiferal tests, the volume was estimated by a comparison to the nearest geometric form (shape). The porosity, effective density in water (DWAT), Corey Shape Factor (CSF), nominal diameter (D_n), maximum projection sphericity (MPS), and operational sphericity (OS) were calculated for each specimen (Table 1 shows the formulas employed).

Settling-Tube Experiments. Settling-velocity experiments were conducted in a clear acrylic tube with an internal diameter of 12 cm and a length of 184 cm (Fig. 9). The tube was filled with distilled water at a temperature of approximately 22°C. The distilled water in the settling tube was allowed to stand for 24 hours prior to use in order for the water to

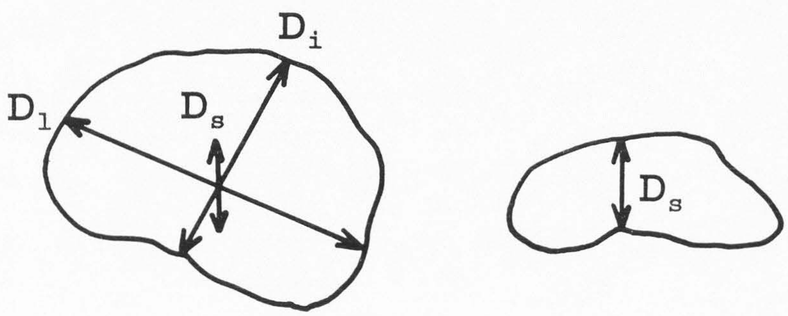

FIGURE 8-Measured test intercepts (also see Table 1).

TABLE 1-Measured and calculated test parameters for evaluation of hydraulic properties.

1. D_s - Minimum intercept
2. D_i - Intermediate intercept
3. D_l - Maximum intercept
4. Weight (mg)
5. Volume (mm^3)
6. Porosity

$$100\% - \frac{\text{Weight}}{\text{Density x Volume}}$$

7. Effective Density in Water (mg/mm^3)

$$\frac{\text{Weight of Water + Weight of Specimen}}{\text{Volume}}$$

8. D_s / D_i and D_i / D_l - Zingg (1935) Shapes
9. Corey Shape Factor (CSF) (Blatt et al., 1980)

$$\frac{D_s}{\sqrt{D_i \times D_l}}$$

10. Nominal Diameter (D_n) - Diameter of sphere with same volume as particle (Wadell, 1932)
11. Maximum Projection Sphericity (MPS) (Sneed and Folk, 1958)

$$\sqrt[3]{\frac{D_s^2}{D_i \times D_l}}$$

12. Operational Sphericity (OS) (Estimate, Krumbein, 1941)

$$\sqrt[3]{\frac{D_s \times D_i}{(D_l)^2}}$$

or

$$\sqrt[3]{\frac{\text{Volume of the Particle}}{\text{Volume of the Circumscribing Sphere}}} \quad \text{(Wadell, 1932)}$$

FIGURE 9-Settling tube used in experiments determining settling velocities of foraminiferal tests.

reach equilibrium conditions and avoid convective flow within the tube. At the bottom of the settling tube, a plastic funnel with a burette was installed and was used to retrieve the settled specimens. The back of the tube was covered with flat black paper to facilitate observation of the settling tests. Three lines were marked on the tube, a zero line 2 cm below the top, and two other lines at 42 cm and 142 cm below the zero line. Wall effects were assumed to be negligible because of the large inner diameter of the settling tube and small specimen sizes.

Prior to the settling experiments, air in foraminiferal test chambers was removed by vacuum-immersing the specimens in water. Settling velocities for tests with chambers filled with air are much slower than those with chambers filled with water because of their different densities. The foraminiferal tests must, therefore, be vacuumed in water to remove air totally before testing so that the maximum settling values can be reached. Pipettes were then used to transfer specimens in water to the settling tube to prevent air invasion of tests. Each specimen was allowed to settle freely through 42 cm to reach its terminal velocity before the settling rate was timed. An electronic stopwatch was used to time specimens to ± 0.01 second as they fell through a total distance of 100 cm. Various types of settling motions (straight, rotation, oscillation from side to side, etc.) were observed and described while specimens descended. Each specimen was settled five times so that settling-velocity means and their confidence intervals could be calculated. The values of time and settling distance recorded in each experiment were converted to velocity in cm/sec. The settling-velocity means of every five were then plotted against various parameters for the different species. These values were also employed in multiple regression analysis against other parameters.

Flume Experiments. Flume experiments were performed in a 3.0-m long by 0.3-m wide by 0.6-m deep open tank (Fig. 10). A gate valve on one side of the flume was connected to the water supply by rubber hose. A 30-cm high, 27-mm diameter PVC pipe in the drain maintained a constant hydraulic head. A group of 20-cm long and 0.55-cm in diameter plastic straws was bound into a cylinder with a diameter of 12 cm and was suspended in front of the gate valve to reduce the turbulence of the flow. A threaded hosecock was used to slowly adjust water flow velocities through the rubber hose. A Marsh-McBirney Model 201D electromagnetic flowmeter was employed to measure changing flow velocities. The precision of measurements was ± 0.01 m/sec. The flume was filled with fresh water 24 hours prior to experiments in order to allow time for the water to reach equilibrium. The temperature of water remained at approximately 22°C throughout the experiments.

At the beginning of each experimental run, a single specimen was placed upon a 10-cm by 10-cm horizontal platform

FIGURE 10-Flume used in experiments determining movement threshold velocities of foraminiferal tests.

which was painted black for visual contrast between foraminiferal specimens and substrate. The platform was located 15 cm above the bottom of the flume and 10 cm directly down flow from the bundle of straws. The sensor of the flowmeter was placed at the same level as the platform in the center of the water column and immediately down flow from the foraminiferal specimens. Two specimen platforms with different surface textures were employed in order to understand the influence of substrate type upon movement thresholds of foraminiferal tests. Platforms utilized in the experiments included one coated with fixed fine sand (0.147 mm) and one coated with fixed coarse sand (0.589 mm).

Water was then injected laterally into the flume, and velocity was slowly increased until the foraminiferal tests moved off the platform boundary. Various parameters such as current velocity at the time of the first movement of foraminiferal test (threshold velocity), and the type of movement (rolling, sliding, saltation, suspension, etc.) were recorded. These values were employed in multiple regression analysis against other parameters.

Quantitative Analyses

All statistical analyses (e.g., confidence interval, regression, and nonparametric tests) involved in this study were done with the computer software of the Number Cruncher Statistical System (NCSS Version 5.03; Hintze, 1990). All cluster analyses performed by this study utilized a PC-based program of hierarchical cluster analysis, the Multi-Variate Statistical Package (MVSP Plus Version 2.0; Kovach, 1990). The Euclidean distance coefficient was used as a dissimilarity measure. Cluster dendrograms were constructed using the Unweighted Pair-Group Method with Arithmetic Averages (UPGMA) (Kovach, 1990).

RESULTS

Insoluble-Residue Content

The greatest differences in total insoluble-residue contents of the 59 sediment samples are between the intertidal and subtidal areas (Mann-Whitney U Test, MWU, $p < 0.001$; Table 2, Figs. 11 and 12). The intertidal and subtidal zones are arbitrarily separated into four subzones: inner flat, 0 - 600 m; middle flat, 600 - 1200 m; outer flat, 1200 - 2500 m; and subtidal, > 2500 m. Within the intertidal zones, no significant correlations between total insoluble content and distance seaward exist. From the inner flat to the subtidal zone (seaward), the total insoluble-residue content generally decreases with increasing distance from shore (Spearman's Rank Correlation Coefficient, SRC, $p < 0.01$), except for a narrow belt near the shore and the Traverse I channel area which have sightly lower total insoluble-residue contents (Figs. 11, 12). Traverse I samples exhibit consistently lower total insoluble-residue values than all other traverses (Wilcoxon Matched Pairs Test, Wilcoxon, $p < 0.05$). The values also exhibit local variation along Traverses V and VI (Fig. 12).

The total calcium carbonate fraction of 54 samples of intertidal sediments averages 10.42% ± 1.78, whereas organic insoluble residue averages 0.35% ± 0.03, and inorganic insoluble residue averages 89.14% ± 1.77. The total calcium car-

TABLE 2-Weight percent insoluble fraction and total $CaCO_3$ of intertidal and subtidal sediments.

Sample #	Distance[a] (m)	% $CaCO_3$	% Organic Insoluble Residue	% Inorganic Insoluble Residue
Traverse I[b]				
T1-45b	0	21.91	0.39	77.70
T1-44b[d]	0	5.25	0.59	94.16
T1-41b	268	14.02	0.20	85.78
T1-40b[d]	402	26.08	0.19	73.73
T1-38b	537	19.96	0.20	79.84
T1-35b[d]	805	21.98	0.19	77.83
T1-34b	805	13.88	0.19	85.93
T1-31b[d]	1074	16.77	0.38	82.85
T1-30b	1074	7.22	0.36	92.41
T1-202	Subtidal	55.93	0.20	43.87
Traverse II[b]				
T2-1b	134	5.10	0.56	93.96
T2-3b	402	5.40	0.38	94.21
T2-5b	671	3.97	0.59	95.43
T2-7b	940	5.59	0.40	94.01
T2-50b	1208	10.12	0.41	89.47
T2-48b	1476	11.66	0.40	87.94
T2-46b	1745	10.83	0.39	84.84
T2-204	Subtidal	50.73	0.24	49.03
Traverse III[b]				
T3-17b	134	9.67	0.41	89.92
T3-15b	402	3.65	0.39	95.96
T3-14b	537	3.94	0.40	95.67
T3-13b	671	10.00	0.39	89.61
T3-12b	805	4.33	0.40	95.28
T3-11b	940	5.47	0.39	94.14
T3-89	1208	6.27	0.39	93.33
T3-84	1476	7.67	0.20	92.14
T3-80	1611	8.44	0.20	91.35
T3-82	1745	8.80	0.38	90.82
T3-206	Subtidal	55.36	0.19	44.44
Traverse IV[b]				
T4-29b	134	9.88	0.40	89.72
T4-27b	402	5.65	0.42	93.92
T4-24b	671	4.78	0.40	94.82
T4-22b	940	6.24	0.59	93.17
T4-20b	1208	10.20	0.60	89.20
T4-18b	1476	8.73	0.40	90.87

TABLE 2-Continued.

Sample #	Distance[a] (m)	% $CaCO_3$	% Organic Insoluble Residue	% Inorganic Insoluble Residue
T4-210	Subtidal	51.90	0.19	47.90
Traverse V[b]				
T5-67b	134	4.85	0.59	94.56
T5-66b	268	6.48	0.60	92.92
T5-65b	402	7.99	0.54	91.47
T5-64b	537	10.60	0.37	89.03
T5-63b	671	10.08	0.57	89.35
T5-62b	805	11.68	0.20	88.13
T5-61b	940	10.65	0.20	89.15
T5-60b	1074	35.65	0.28	64.08
T5-59b	1208	12.57	0.41	87.02
T5-208	Subtidal	53.58	0.49	45.94
Traverse VI[c]				
T6-550b	100	9.36	0.20	90.44
T6-548b	300	9.14	0.40	90.46
T6-546b	500	25.72	0.20	74.08
T6-544b	700	8.40	0.20	91.40
T6-542b	900	7.18	0.20	92.62
T6-540b	1100	6.76	0.20	93.04
T6-538b	1300	7.90	0.40	91.70
T6-536b	1500	6.99	0.40	92.61
T5-534b	1700	8.42	0.20	91.38
T6-532b	1900	8.34	0.20	91.46
T6-530b	2100	9.92	0.20	89.88
T6-528b	2300	23.78	0.20	76.02
T6-526b	2500	6.95	0.20	92.85

[a] Distance seaward from the shore.
[b] Samples from Traverses I, II, III, IV, V were collected in July 1991.
[c] Samples from Traverse VI were collected in July 1992.
[d] Samples collected from the middle of the channel.

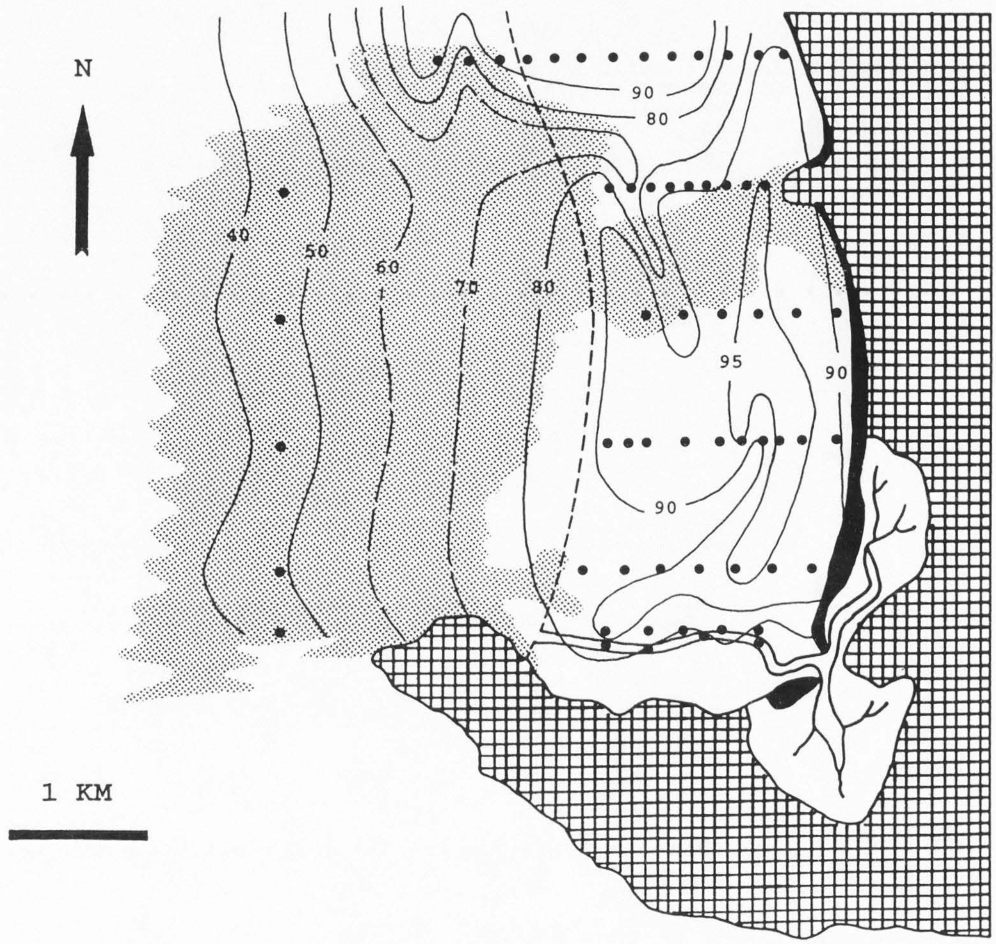

FIGURE 11-Contour map of percent total insoluble-residue content in sediments of Bahia la Choya, Mexico (modified from Meldahl, 1990; stippling indicates exposures of lithified Pleistocene sediments; dots show sample locations; approximate low water indicated by dashed line).

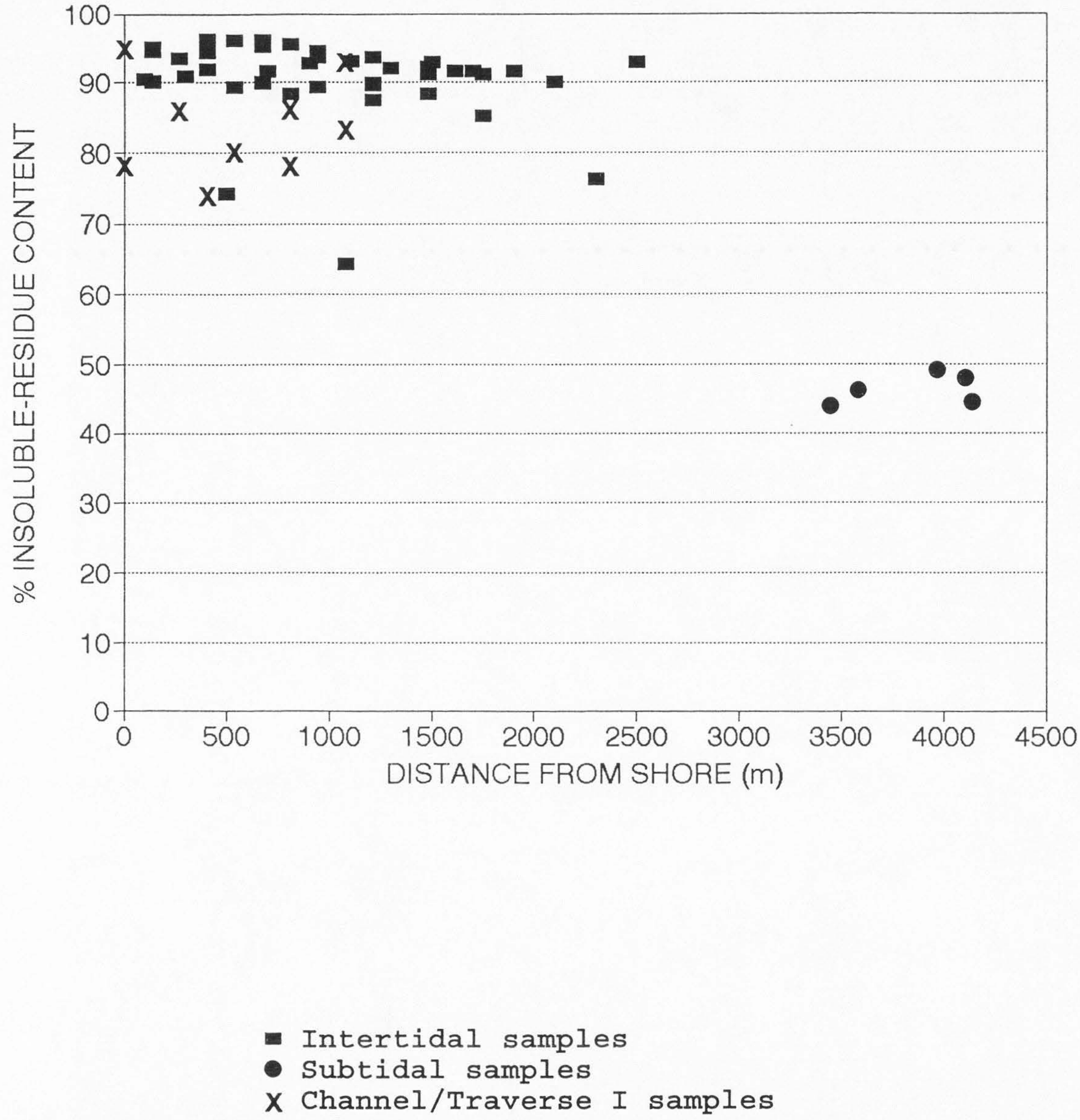

FIGURE 12-Plot of percent total insoluble-residue content versus distance seaward from shore for sediments from Bahia la Choya, Mexico.

bonate fraction of subtidal sediments averages 53.50% ± 2.75, whereas organic insoluble residue averages 0.26% ± 0.15, and other insoluble residue averages 46.24% ± 2.74. Q-mode cluster analysis of percent mineralogical composition data (Table 2) produced a dendrogram (Fig. 13) that identifies three groups which are present in the study area, representing channel, intertidal, and subtidal zones (with a few exceptions). Within the intertidal group, Traverse VI samples are most distinct from the others.

Constituent-Particle Composition

Thin-section studies reveal that, according to the means of all point-counted samples, the Holocene sediment samples consist of two major grain types: quartz (67.9% ± 15.0) and unidentified molluscan shell fragments (20.3% ± 11.7); three minor grain types: micritized grains (6.2% ± 3.5), composite grains (2.1% ± 1.0), and feldspar (1.0% ± 0.5); and trace amounts of other grain components, including heavy minerals (0.9% ± 0.5), bryozoans (0.8% ± 0.9), Foraminifera (0.2% ± 0.2), bivalves (0.2% ± 0.3), barnacles (0.2% ± 0.3), gastropods (0.1% ± 0.2), and unidentified grains (0.1% ± 0.1) (Table 3). These data indicate that percentage compositions of constituent particles in the intertidal samples are much different from those of subtidal samples (Table 4, Fig. 14). Within the intertidal zone, quartz in the sediment decreases while unidentified molluscan shell fragments increase from

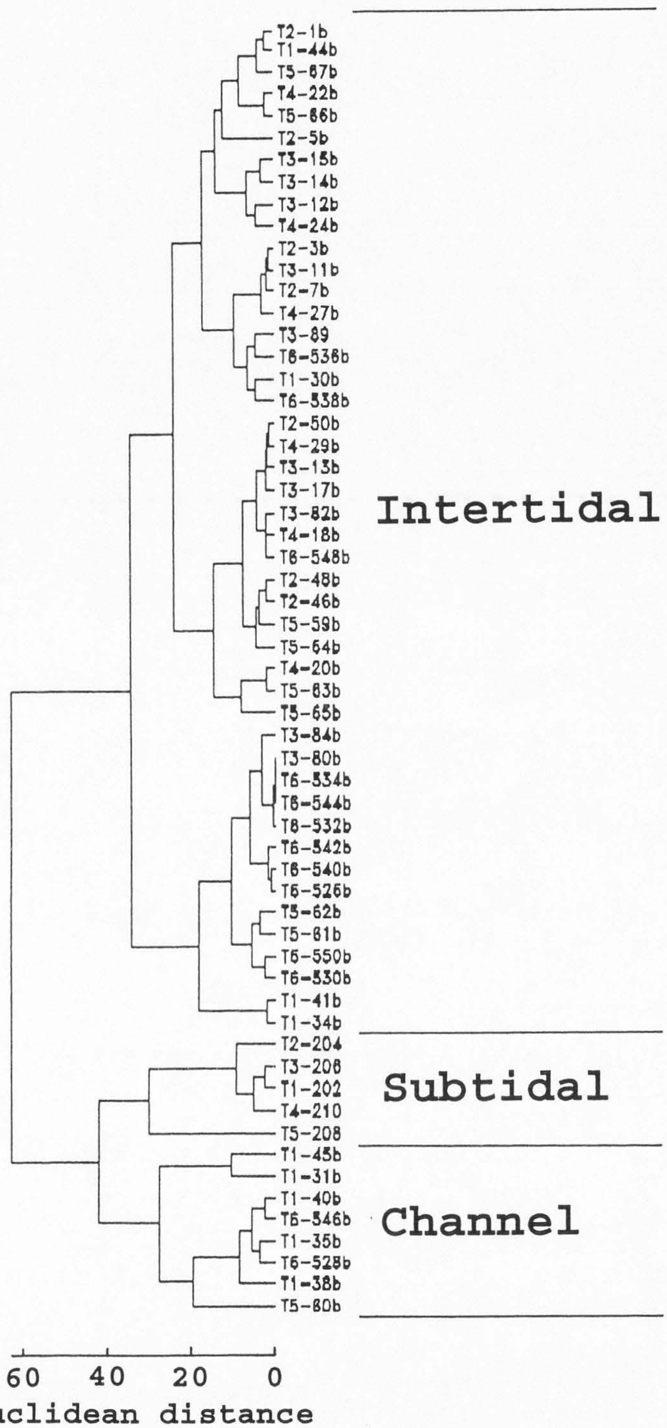

FIGURE 13-Cluster dendrogram, based upon analysis of total insoluble-residue contents of sediment samples, shows three major environmental zones. Dendrogram uses data in Table 2, Euclidean distance, and UPGMA clustering method.

TABLE 3-Sediment constituent composition (%) for Traverses II, III, V, with means and 95% confidence intervals. All samples were collected in July 1991.

Sample #	Distance[a] (m)	Foraminifera	Bivalve	Gastropod	Bryozoan	Barnacle	Micritized Grain	Shell Fragment	Quartz	Feldspar	Heavy Mineral	Composite Grain	Unidentified Grain
Traverse II													
T2-1b	134	0.0	0.3	0.0	0.0	0.0	3.7	4.7	82.3	3.0	1.7	4.3	0.0
T2-7b	940	0.0	0.0	0.0	0.0	0.0	2.0	14.3	78.3	0.7	0.7	3.7	0.3
T2-46b	1745	0.7	0.7	0.0	0.0	0.0	0.7	19.0	72.3	1.0	0.3	5.3	0.0
T2-204	Subtidal	0.8	1.5	0.0	4.5	1.3	20.5	43.0	26.5	0.3	0.5	1.0	0.3
Traverse III													
T3-17b	134	0.0	0.0	0.0	0.0	0.0	4.0	6.3	87.0	0.3	1.3	1.0	0.0
T3-11b	940	0.0	0.0	0.0	0.0	0.0	5.3	6.3	85.3	0.3	0.3	2.3	0.0
T3-82	1745	0.0	0.0	0.0	0.8	0.0	7.3	5.8	83.5	0.5	0.8	1.5	0.0
T3-206	Subtidal	0.0	0.0	0.0	2.0	1.0	11.0	52.3	32.3	0.7	0.0	0.7	0.0
Traverse V													
T5-67b	134	0.0	0.0	0.0	0.0	0.0	5.0	5.3	86.0	2.3	0.3	1.0	0.0
T5-62b	805	0.3	0.0	0.0	0.0	0.0	4.3	11.3	79.0	1.0	1.7	2.3	0.0
T5-59b	1208	0.3	0.0	0.0	0.0	0.0	0.7	24.0	72.0	1.0	0.3	1.7	0.0
T5-208	Subtidal	0.0	0.0	1.3	2.3	0.3	9.7	51.7	30.3	1.3	2.3	0.3	0.3
Mean		0.2	0.2	0.1	0.8	0.2	6.2	20.3	67.9	1.0	0.9	2.1	0.1
(95% C.I.)		(±0.2)	(±0.3)	(±0.2)	(±0.9)	(±0.3)	(±3.5)	(±11.7)	(±15.0)	(±0.5)	(±0.5)	(±1.0)	(±0.1)

[a] Distance seaward from the shore.

TABLE 4-Sediment constituent compositions (%) with means and 95% confidence intervals for intertidal and subtidal zones (average of three traverses).

Location	Intertidal				Subtidal
	Inner	Middle	Outer		
Distance (m x 100) (seaward from shore)	0 - 6	6 - 12	12 - 25		> 25
Sample Size (n)	3	3	3		3
Constituent				Mean (Intertidal)	
Foraminifera	0.0	0.1 ± 0.4	0.3 ± 0.9	0.1 ± 0.2	0.3 ± 1.1
Bivalve	0.1 ± 0.4	0.0	0.2 ± 1.0	0.1 ± 0.2	0.5 ± 2.2
Gastropod	0.0	0.0	0.0	0.0	0.4 ± 1.9
Bryozoan	0.0	0.0	0.3 ± 1.1	0.1 ± 0.2	2.9 ± 3.4
Barnacle	0.0	0.0	0.0	0.0	0.9 ± 1.3
Micritized Grain	4.2 ± 1.7	3.9 ± 4.2	2.9 ± 9.5	3.7 ± 1.7	13.7 ± 14.7
Shell Fragment	5.4 ± 2.0	10.6 ± 10.0	16.3 ± 23.4	10.8 ± 5.3	49.0 ± 12.9
Quartz	85.1 ± 6.2	80.9 ± 9.6	75.9 ± 16.3	80.6 ± 4.3	29.7 ± 7.3
Feldspar	1.9 ± 3.5	0.7 ± 0.9	0.8 ± 0.7	1.1 ± 0.7	0.8 ± 1.3
Heavy Mineral	1.1 ± 1.8	0.9 ± 1.8	0.5 ± 0.7	0.8 ± 0.5	0.9 ± 3.0
Composite Grain	2.1 ± 4.7	2.8 ± 2.0	2.8 ± 5.3	2.6 ± 1.2	0.7 ± 0.9
Unidentified	0.0	0.1 ± 0.4	0.0	0.0	0.2 ± 0.4

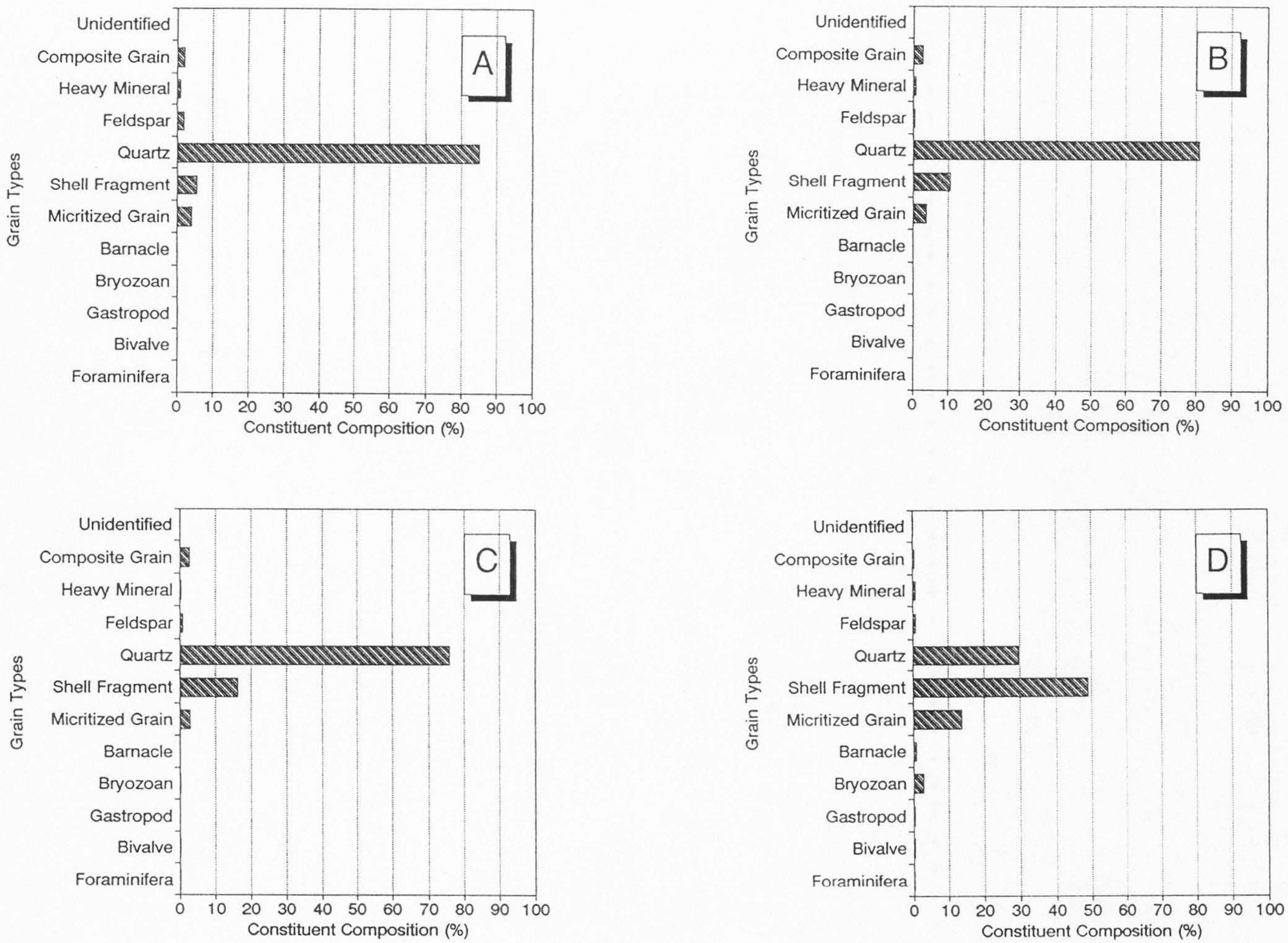

FIGURE 14-The mean constituent composition (%) of sediment samples determined by thin-section point-counts from (A) inner flat, (B) middle flat, (C) outer flat, and (D) subtidal, average of 3 traverses (Table 4).

the inner to outer flat zones (Table 4). Q-mode cluster analysis resulted in four major groups, which are well-defined associations representing sediments of varying composition from inner, middle, and outer intertidal zones, and the subtidal zone (with a few exceptions)(Fig. 15).

The composition of the Pleistocene rock samples, as determined by thin-section analysis, includes three major grain types: fine-grained carbonate matrix (53.3 ± 10.0), quartz (25.4 ± 8.9), and unidentified molluscan shell fragments (12.5 ± 9.7); five minor grain types: unidentified grains (2.1 ± 1.0), micritized grains (1.9 ± 1.9), bryozoans (1.3 ± 1.3), feldspar (1.1 ± 0.9), and composite grains (1.0 ± 0.8); and trace amount of other grain components: heavy minerals (0.6 ± 0.7), gastropods (0.5 ± 1.1), barnacles (0.4 ± 0.8), and bivalves (0.1 ± 0.3)(Table 5). Q-mode cluster analysis (Fig. 16) shows that two groupings are observed among three vertical sampling positions within the Pleistocene outcrops (with a few exceptions).

Texture

Forty-two sediment samples from six traverse lines were used for grain-size analysis. The results are shown in Tables 6 and 7 and Figures 17, 18, and 19. Upon the whole, the intertidal sediment has a fine mean grain size (M_z = 2.73 ± 0.15), is moderately well sorted (IGSD = 0.65 ± 0.09), and is coarse skewed (SK_i = -0.19 ± 0.07). By comparison, the sub-

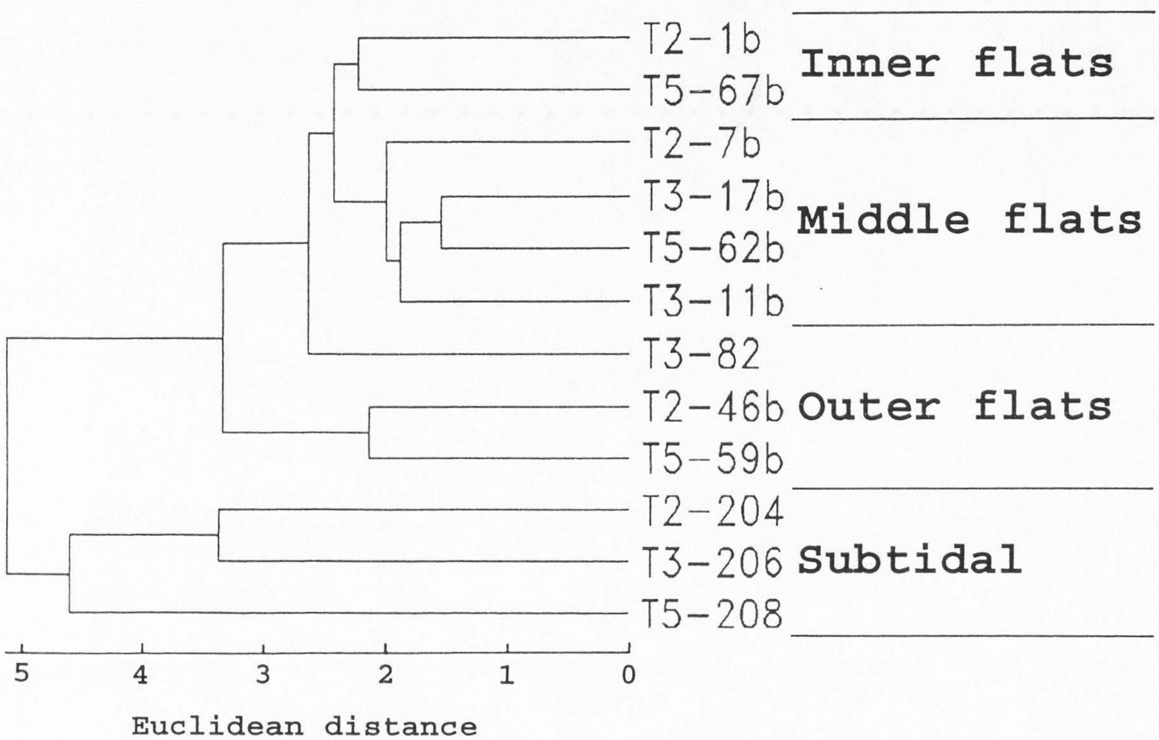

FIGURE 15-Cluster dendrogram, based upon analysis of constituent particle composition of sediment samples, shows four major environmental zones. Dendrogram uses data in Table 3, Euclidean distance, and UPGMA clustering method.

TABLE 5-Pleistocene rock constituent composition (%), with means and 95% confidence intervals.

Sample #	Position	Bivalve	Gastropod	Bryozoan	Barnacle	Micritized Grain	Shell Fragment	Quartz	Feldspar	Heavy Mineral	Composite Grain	Unidentified Grain	Matrix
P4	Top	1.3	5.0	4.5	0.0	1.0	13.5	21.3	0.3	0.5	2.5	4.3	46.0
P5	Bottom	0.0	0.0	0.0	0.0	7.3	3.7	25.0	0.0	0.0	2.7	2.0	59.3
P8	Top	0.0	0.0	0.0	0.0	0.0	27.7	17.7	1.0	0.3	0.7	0.3	52.3
P9	Middle	0.0	0.0	3.0	0.0	3.3	8.3	6.0	0.0	0.0	0.0	4.0	75.3
P10	Bottom	0.0	0.0	0.0	0.0	1.0	26.3	9.7	0.0	0.0	0.3	2.7	60.0
P30	Top	0.0	0.0	0.0	0.0	0.0	4.3	33.3	2.0	1.0	0.0	1.7	57.7
P31	Middle	0.0	0.0	3.3	0.0	0.0	0.7	28.7	1.3	0.0	1.0	1.3	63.7
P32	Bottom	0.0	0.0	1.8	0.0	0.5	0.5	37.5	0.3	0.0	2.0	1.3	56.3
P35	Top	0.0	0.0	0.0	0.0	0.0	38.3	27.3	3.8	2.8	0.0	0.5	27.5
P36	Middle	0.0	0.0	0.0	3.7	5.7	1.3	47.3	2.7	1.3	0.3	2.7	35.0
Mean		0.1	0.5	1.3	0.4	1.9	12.5	25.4	1.1	0.6	1.0	2.1	53.3
(95% C.I.)		(±0.3)	(±1.1)	(±1.3)	(±0.8)	(±1.9)	(±9.7)	(±8.9)	(±0.9)	(±0.7)	(±0.8)	(±1.0)	(±10.0)

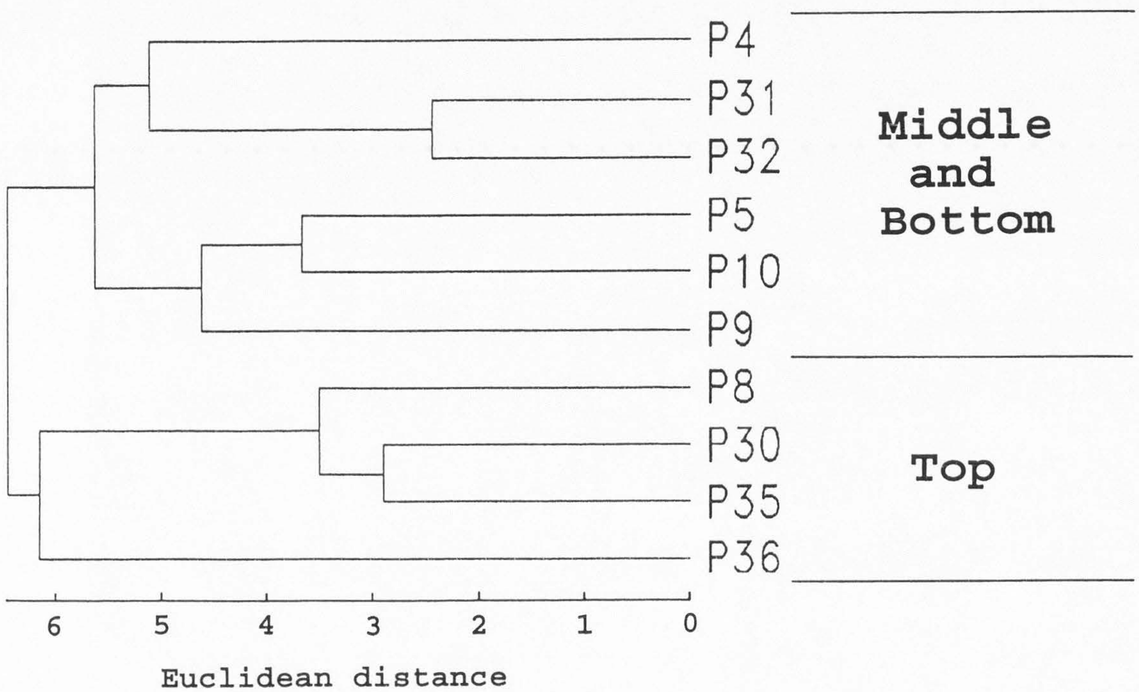

FIGURE 16-Cluster dendrogram, based upon analysis of constituent particle composition of Pleistocene rock samples, shows that two groups are present among three vertical positions. Dendrogram uses data in Table 5, Euclidean distance, and UPGMA clustering method.

TABLE 6-Median grain size (M_d), mean grain size (M_z), sorting (IGSD), and skewness (SK_i) for sediment samples (after Folk, 1968). Median, mean, and sorting are in phi units.

Sample #	Distance[a] (m)	Median (M_d)	Mean (M_z)	Sorting (IGSD)	Skewness (SK_i)
Traverse I[b]					
T1-45b	0	1.67	1.43	1.27	-0.19
T1-34b	805	2.06	1.74	1.42	-0.30
T1-30b	1074	2.78	2.73	0.74	-0.27
T1-202	Subtidal	1.13	1.15	1.30	0.03
Traverse II[b]					
T2-1b	134	2.47	2.66	0.92	0.21
T2-3b	402	3.35	3.22	0.62	-0.35
T2-5b	671	3.02	2.85	0.61	-0.34
T2-7b	940	2.72	2.69	0.59	-0.05
T2-50b	1208	2.32	2.14	0.83	-0.43
T2-48b	1476	2.25	2.12	0.76	-0.39
T2-46b	1745	2.10	2.06	0.71	-0.19
T2-204	Subtidal	1.41	1.31	1.47	-0.10
Traverse III[b]					
T3-17b	134	3.27	2.86	1.08	-0.54
T3-15b	402	2.47	2.63	0.53	0.44
T3-13b	671	2.46	2.55	0.97	-0.11
T3-11b	940	3.01	2.96	0.47	-0.15
T3-89	1208	2.65	2.66	0.49	0.00
T3-84	1476	2.44	2.49	0.51	0.19
T3-82	1745	2.27	2.21	0.41	-0.23
T3-206	Subtidal	1.25	1.21	1.20	-0.01
Traverse IV[b]					
T4-29b	134	3.18	2.85	0.91	-0.47
T4-22b	940	2.64	2.70	0.60	-0.07
T4-18b	1476	2.39	2.37	0.52	-0.10
T4-210	Subtidal	1.84	1.75	1.10	-0.13
Traverse V[b]					
T5-67b	134	2.52	2.55	0.37	0.16
T5-66b	268	3.15	3.11	0.46	-0.18
T5-61b	940	3.07	3.00	0.55	-0.33
T5-59b	1208	2.84	2.85	0.53	-0.09
T5-208	Subtidal	1.75	1.64	1.41	-0.16

TABLE 6-Continued.

Sample #	Distance[a] (m)	Median (M_d)	Mean (M_z)	Sorting (IGSD)	Skewness (SK_i)
Traverse VI[c]					
T6-550b	100	3.32	3.24	0.76	-0.22
T6-548b	300	3.36	3.31	0.64	-0.17
T6-546b	500	2.52	2.25	1.02	-0.36
T6-544b	700	3.04	3.01	0.47	-0.10
T6-542b	900	3.13	3.10	0.41	-0.07
T6-540b	1100	3.18	3.15	0.34	-0.12
T6-538b	1300	3.15	3.11	0.43	-0.24
T6-536b	1500	3.19	3.17	0.38	-0.16
T6-534b	1700	3.14	3.08	0.47	-0.35
T6-532b	1900	3.19	3.18	0.37	-0.13
T6-530b	2100	3.20	3.15	0.60	-0.39
T6-528b	2300	3.21	2.68	1.09	-0.68
T6-526b	2500	3.18	3.20	0.36	-0.11

[a] Distance seaward from the shore.
[b] Samples from Traverses I, II, III, IV, V, were collected in July 1991.
[c] Samples from Traverse VI were collected in July 1992.

TABLE 7-Average values of median grain size (M_d), mean grain size (M_z), sorting (IGSD), and skewness (SK_i) for intertidal and subtidal sediment samples, as well as their 95% confidence intervals. Median, mean, and sorting are in phi units.

Location	Intertidal						Subtidal
Traverse #	I	II	III	IV	V	VI	
Textural Parameters							
Median (M_d)	2.17±1.73	2.60±0.41	2.65±0.33	2.74±1.01	2.90±0.45	3.14±0.12	1.48±0.39
Mean (M_z)	1.97±1.69	2.53±0.40	2.62±0.23	2.64±0.61	2.88±0.39	3.05±0.17	1.41±0.33
Sorting (IGSD)	1.14±0.88	0.72±0.11	0.64±0.25	0.68±0.52	0.48±0.13	0.56±0.15	1.30±0.19
Skewness (SK_i)	-0.25±0.14	-0.22±0.21	-0.06±0.29	-0.21±0.56	-0.11±0.33	-0.24±0.10	-0.07±0.10

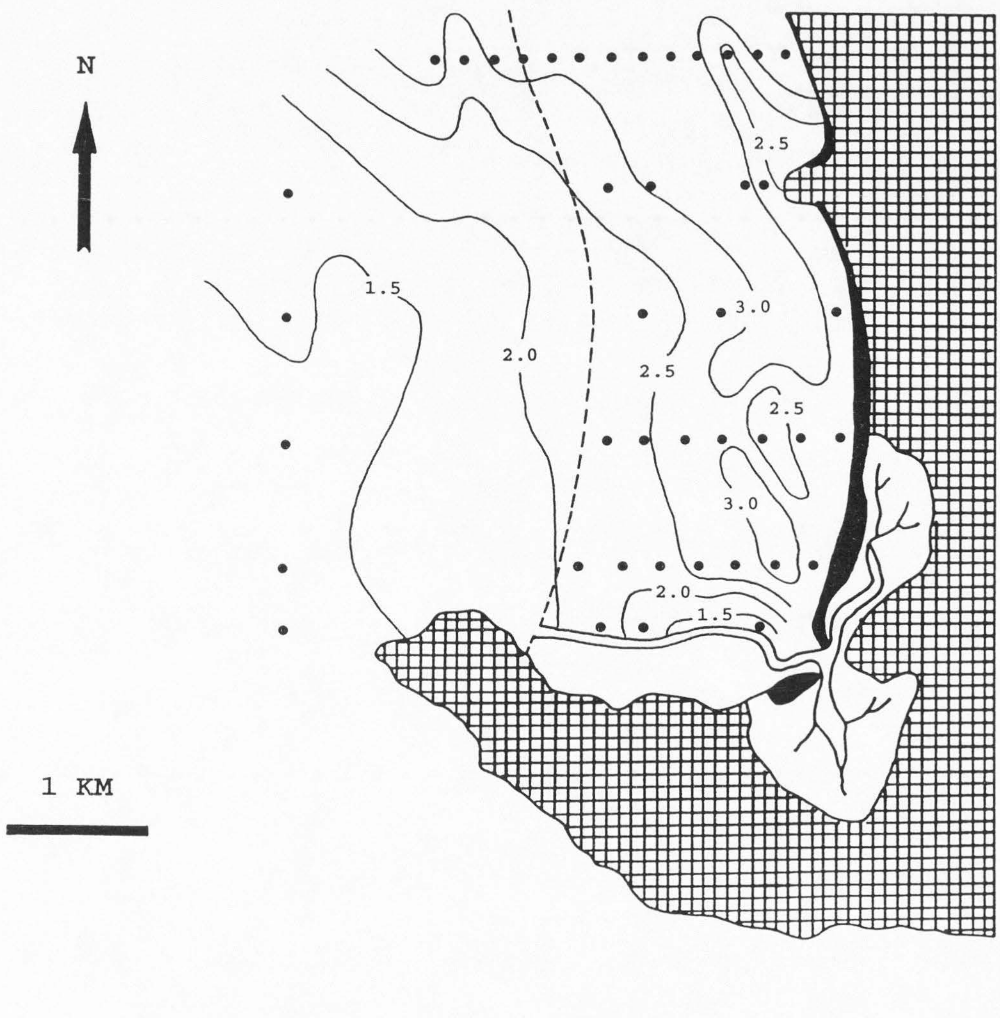

FIGURE 17-Contour map of mean grain size (M_z) in sediments of Bahia la Choya, Mexico (modified from Meldahl, 1990; dots show sample locations; approximate low water indicated by dashed line).

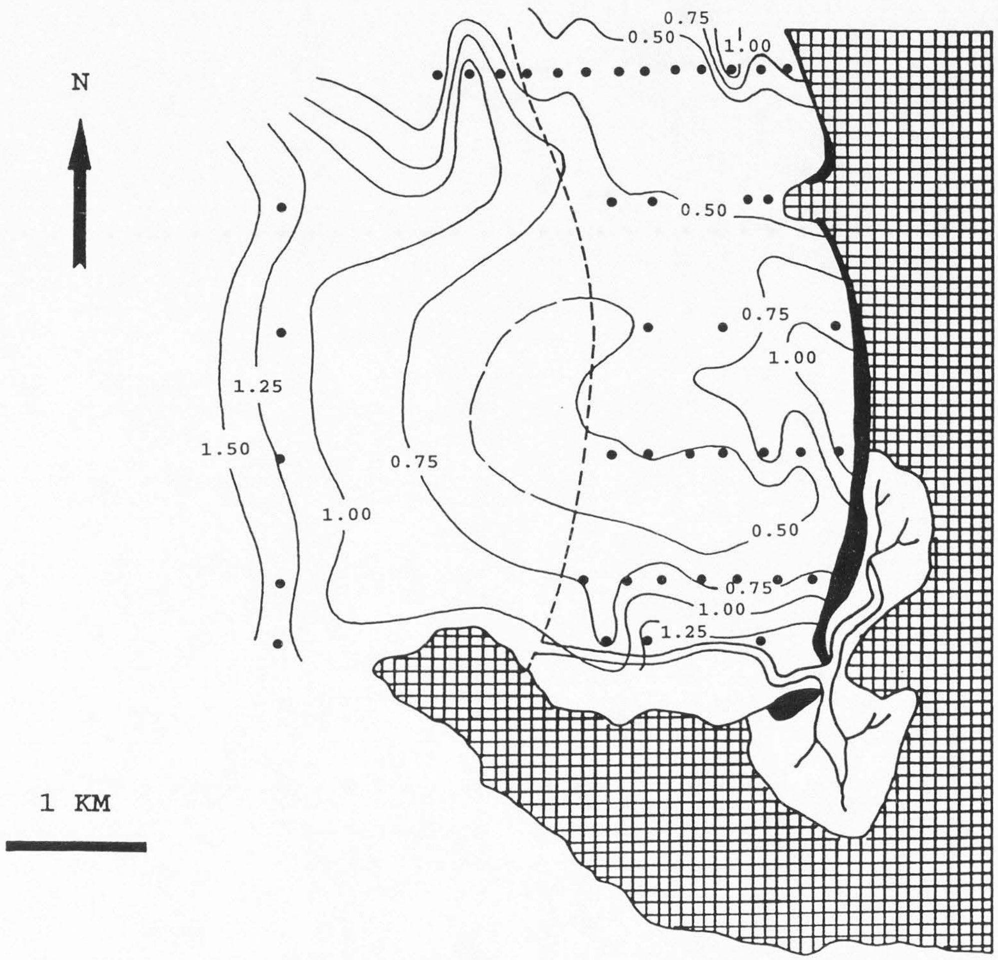

FIGURE 18-Contour map of sorting (IGSD) in sediments of Bahia la Choya, Mexico (modified from Meldahl, 1990; dots show sample locations; approximate low water indicated by dashed line).

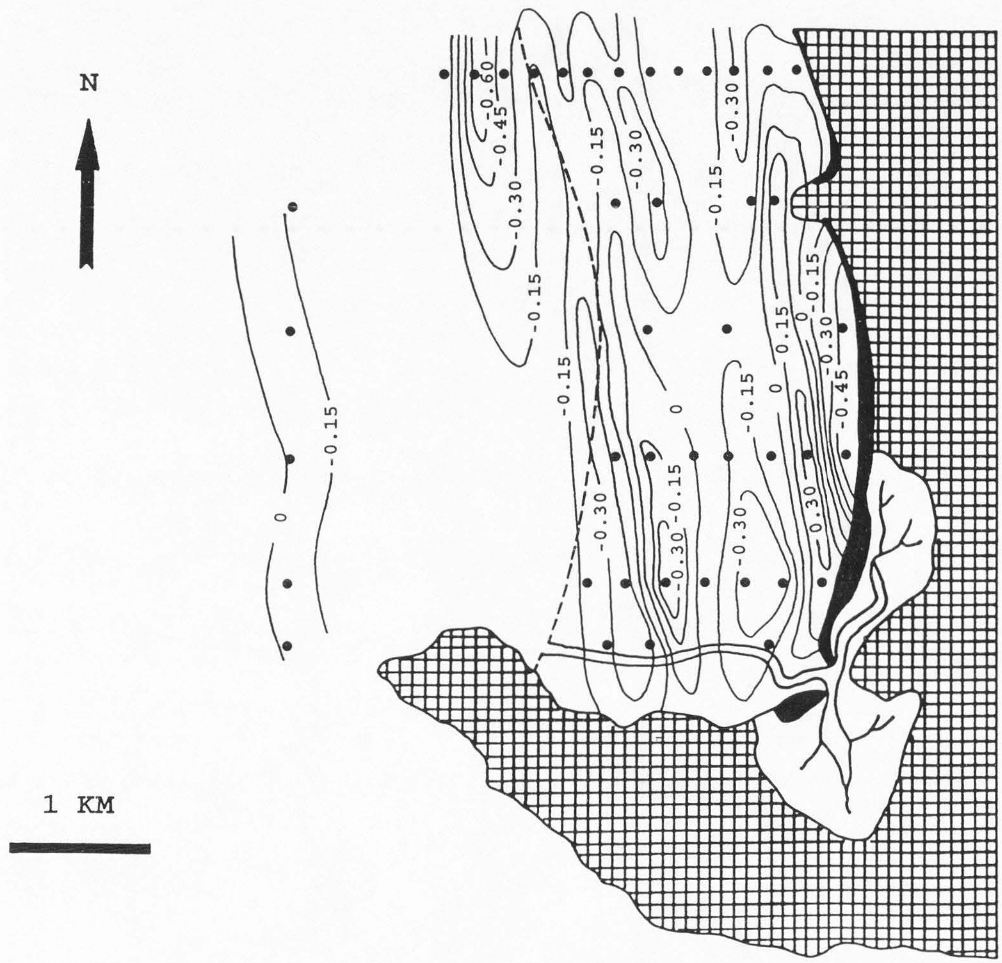

FIGURE 19-Contour map of skewness (SK_i) in sediments of Bahia la Choya, Mexico (modified from Meldahl, 1990; dots show sample locations; approximate low water indicated by dashed line).

tidal sediment has a medium mean grain size (M_z = 1.41 ± 0.33), is poorly sorted (IGSD = 1.30 ± 0.19), and is nearly symmetrically skewed (SK_i = -0.07 ± 0.10). The differences in mean grain size between intertidal and subtidal samples are significant (MWU, $p < 0.001$). Mean grain size (M_z) shows a tendency to increase across the intertidal zone to the subtidal zone (Fig. 20). Traverse VI is an exception to this trend and shows little change in M_z with increasing depth (SRC, $p < 0.07$ for all Traverses; SRC, $p < 0.002$ for Traverses I - V only). Overall, intertidal sediment samples from Traverse VI are finer grained than those of the other traverses (Wilcoxon, $p < 0.01$). Mean grain size in the intertidal zone also increases southward from Traverse VI (SRC, $p < 0.002$)(Table 6, Fig. 20). Sorting and skewness show no significant offshore trend through the entire area sampled (Fig. 21). However, sediment sorting in the intertidal zone has an apparent S-N trend, from poorly sorted or moderately sorted in Traverses I and II to moderately well sorted or well sorted in Traverses III, IV, V, VI (SRC, $p < 0.002$) (Table 7, Fig. 18).

Based on plots of the median grain size (M_d) against sorting (IGSD) and skewness (SK_i), and plots of the mean grain size (M_z) against sorting (IGSD) and skewness (SK_i), the sediments of the study area fall generally into two groups with few exceptions (Fig. 22). Q-mode cluster analysis of sediment textural values included in Table 6 shows that two

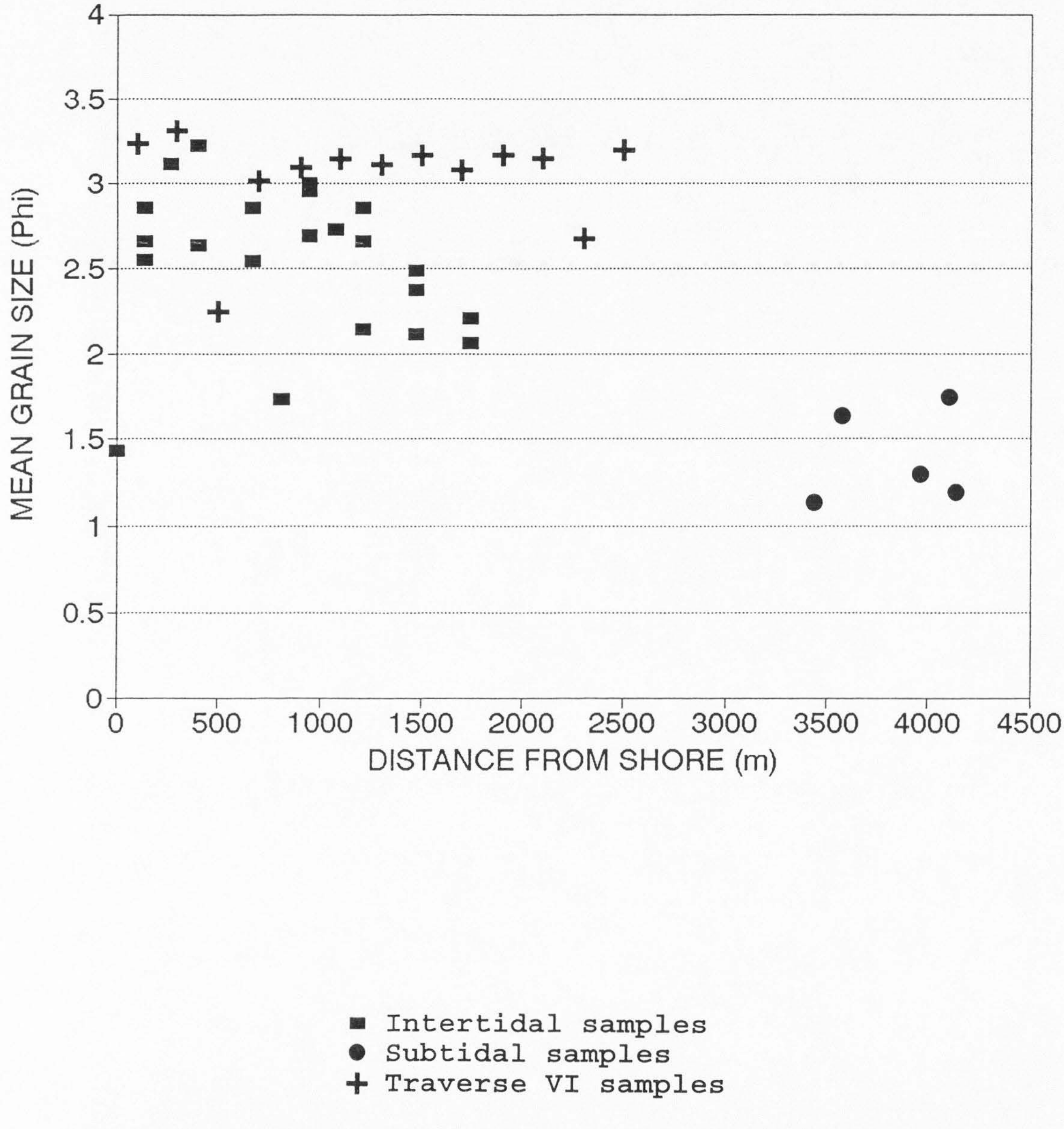

FIGURE 20-Plot of mean grain size versus distance seaward from shore for sediments from Bahia la Choya, Mexico.

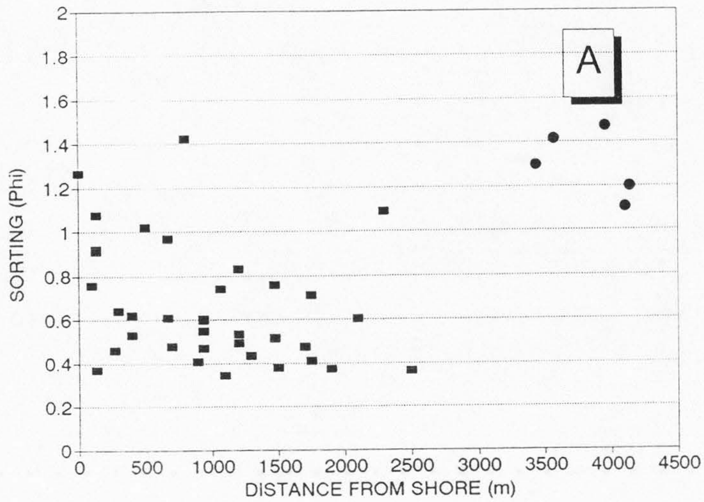

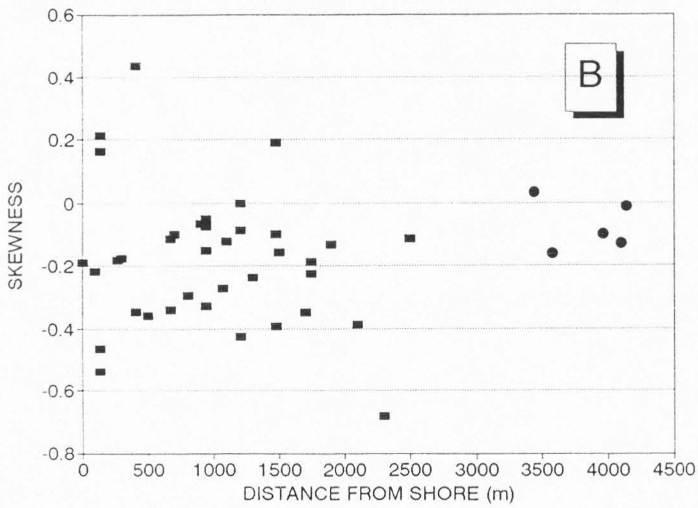

▪ Intertidal samples
• Subtidal samples

FIGURE 21-Plots of (A) sorting and (B) skewness versus distance seaward from shore for sediments from Bahia la Choya, Mexico.

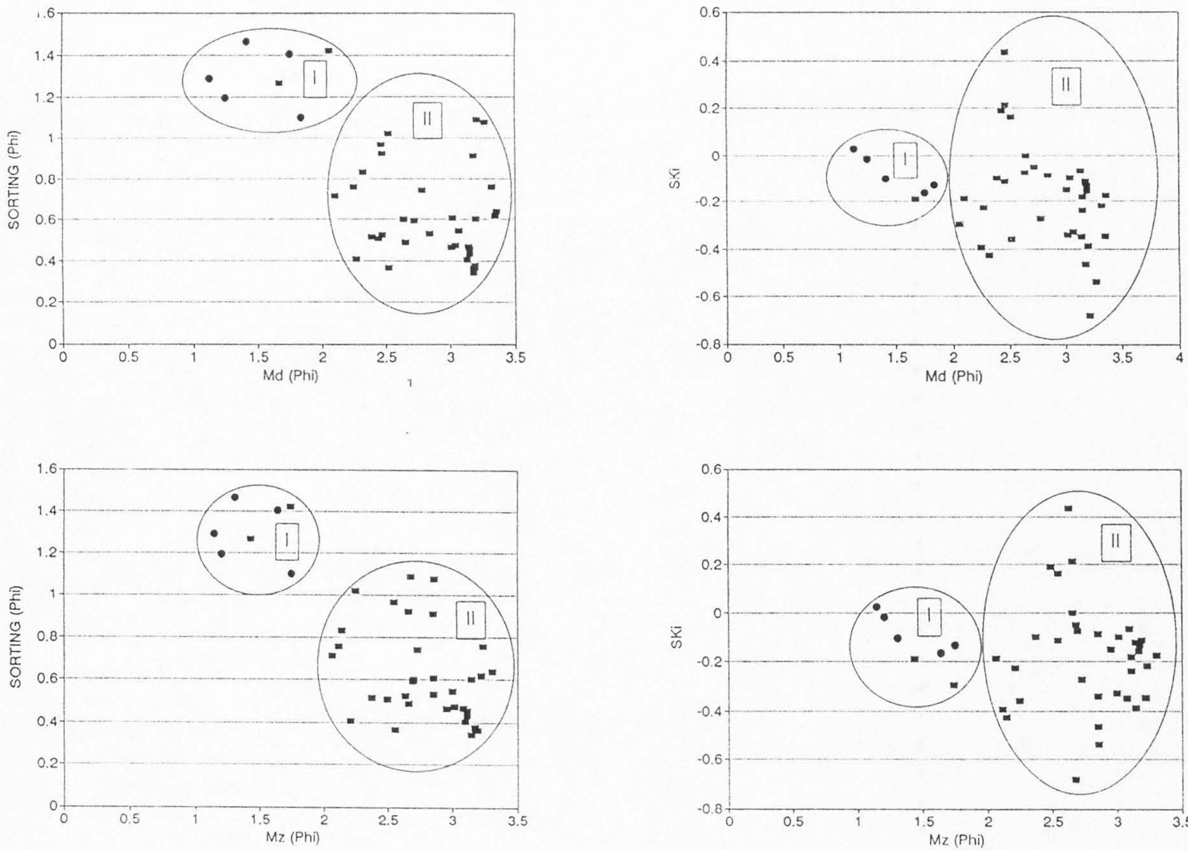

▪ Intertidal sediment samples
• Subtidal sediment samples

FIGURE 22-Sediment groups in Bahia la Choya, Mexico, based on plots of median grain size (M_d) against both sorting (IGSD) and skewness (SK_i), and on plots of mean grain size (M_z) against both sorting (IGSD) and skewness (SK_i). Group I represents sediment samples from the subtidal zone with only a few exceptions. Group II represents sediment samples from the intertidal zone.

groups representing intertidal and subtidal are present in the study area (with few exceptions)(Fig. 23). Within the intertidal group, some S-N trends can also be seen, resulting in south and north subgroups (Fig. 23).

Distribution of Living and Dead Benthonic Foraminifera

A total of 24 stained sediment samples collected in July 1991 was used to determine living and dead populations of benthonic Foraminifera (Tables 8 and 9). These samples were spaced along a series of five traverse lines I, II, III, IV, and V, which gave relatively good coverage for the entire study area (Fig. 24). Sediment samples chosen cover inner flat, middle flat, outer flat, and subtidal environments. Samples of shells, rubble, and macrophytes yielded few or no foraminiferal tests.

The living populations per milliliter of sieved sediment (-2 to +4 phi) are very small, being much less than 1/ml in the study area (Fig. 25). In contrast, the numbers of dead Foraminifera per milliliter are larger, and vary between 3/ml and 52/ml (Fig. 26). The distributions of total populations (living and dead) of benthonic Foraminifera per ml of sieved sediment generally change seaward from small populations to large populations, except in the 1500 - 2000 m seaward zone, and are strikingly similar to the distributions of the dead populations because of the small populations of living Fo-

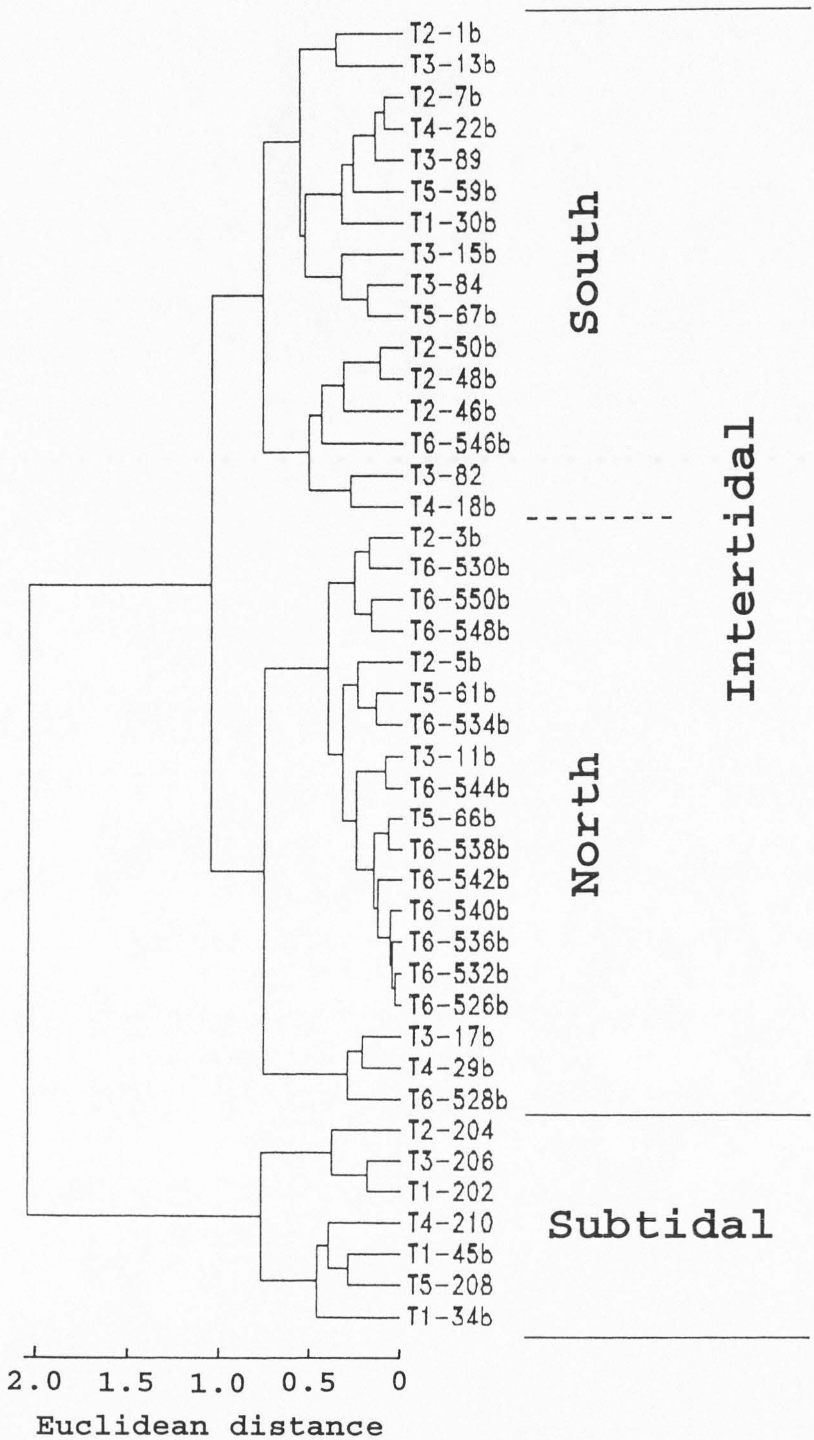

FIGURE 23-Cluster dendrogram, based upon analysis of sediment textural values, shows two major environmental zones. Dendrogram uses data in Table 6, Euclidean distance, and UPGMA clustering method.

TABLE 8-Distribution of living and dead benthonic Foraminifera. All samples were collected in July 1991.

SAMPLE #	Distance[a] (m)	LIVING # (L)	DEAD #	Total # (T)	Living # /ml	Dead # /ml	Total # /ml	L #/T # (%)
Traverse I								
T1-45	0	0	28	28	0	0.90	0.90	0
T1-39	402	0	767	767	0	11.25	19.18	0
T1-34	805	0	450	450	0	14.52	14.52	0
Traverse II								
T2-1	134	2	17	19	0.06	0.49	0.54	11.11
T2-4	541	3	230	233	0.08	5.75	5.83	1.37
T2-7	940	3	798	801	0.08	22.17	22.25	0.36
T2-49	1342	37	1780	1817	0.93	44.50	45.43	2.05
T2-46	1745	6	67	73	0.18	1.97	2.15	8.37
T2-203	Subtidal	6	2426	2432	0.15	60.65	60.80	0.25
Traverse III								
T3-17	134	19	126	145	0.55	3.64	4.19	13.13
T3-14	541	0	68	68	0	1.70	1.70	0
T3-11	940	5	349	354	0.14	9.48	9.62	1.46
T3-85	1342	1	1111	1112	0.03	27.78	27.80	0.11
T3-81	1745	0	139	139	0	4.03	4.03	0
T3-205	Subtidal	10	1561	1571	0.23	36.30	36.53	0.63
Traverse IV								
T4-29	134	0	295	295	0	9.52	9.52	0
T4-25	541	0	284	284	0	7.10	7.10	0
T4-22	940	0	384	384	0	11.46	11.46	0
T4-18	1476	0	109	109	0	3.30	3.30	0
Traverse V								
T5-67	134	0	94	94	0	2.67	2.67	0
T5-65	402	0	989	989	0	24.73	24.73	0
T5-62	805	3	488	491	0.08	13.75	13.83	0.58
T5-59	1208	0	571	571	0	15.35	15.35	0
T5-207	Subtidal	12	2247	2259	0.31	57.91	58.22	0.53

[a] Distance seaward from the shore.

TABLE 9-Distribution of living and dead benthonic Foraminifera in different seaward zones -- means of samples from five traverses. All samples were collected in July 1991.

Distance[a] (m)	N[b]	Living # /ml	Dead # /ml	Total # /ml	L #/T # (%)
0-200	5	0.12	3.44	3.56	3.61
200-600	5	0.02	10.11	11.71	0.13
600-1000	5	0.06	14.28	14.34	0.44
1000-1500	4	0.24	22.73	22.97	2.97
1500-2000	2	0.09	3.00	3.09	2.83
Subtidal (>2500)	3	0.23	51.62	51.85	0.45

[a] Distance seaward from the shore.
[b] N represents the number of individual samples.

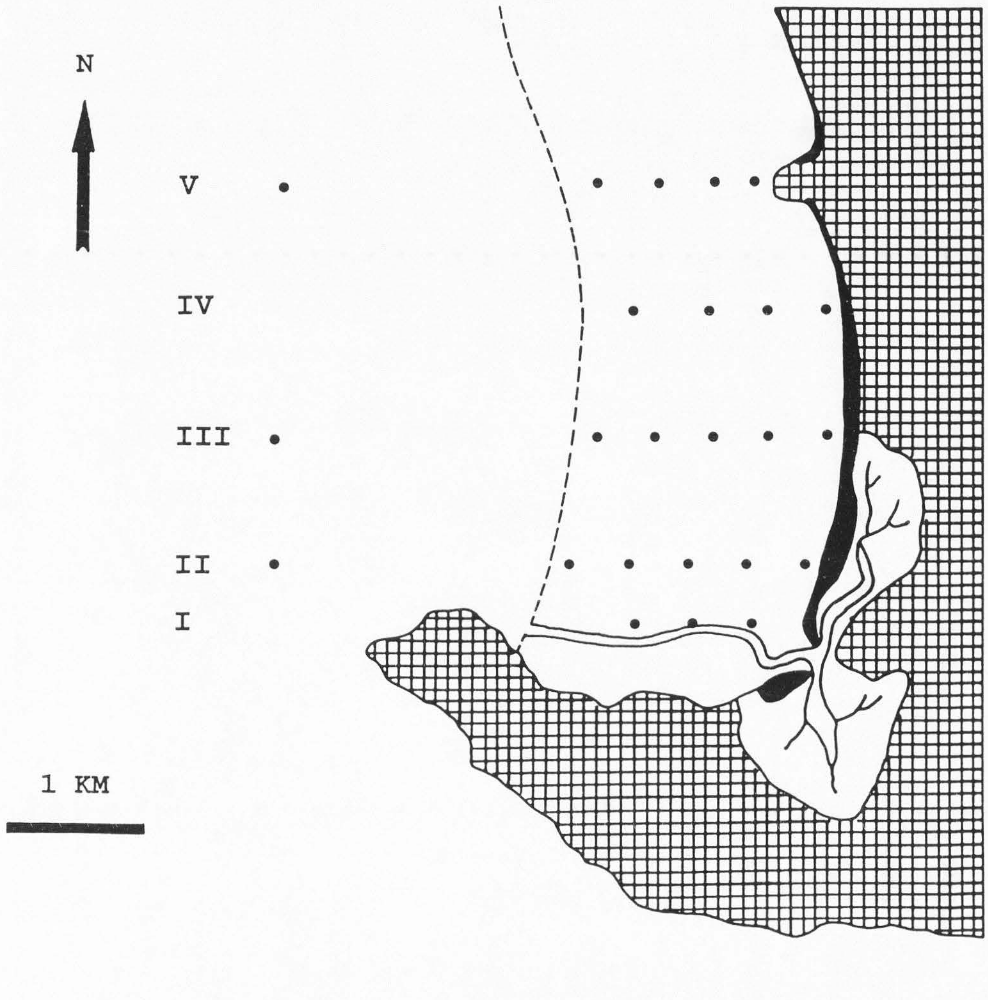

FIGURE 24-Locations of sediment samples used for distribution studies of benthonic Foraminifera (modified from Meldahl, 1990; dots show sample locations). Traverse codes: I = Traverse A-A', II = Traverse B-B', III = Traverse C-C', IV = Traverse D-D', and V = Traverse E-E' (Fig. 1).

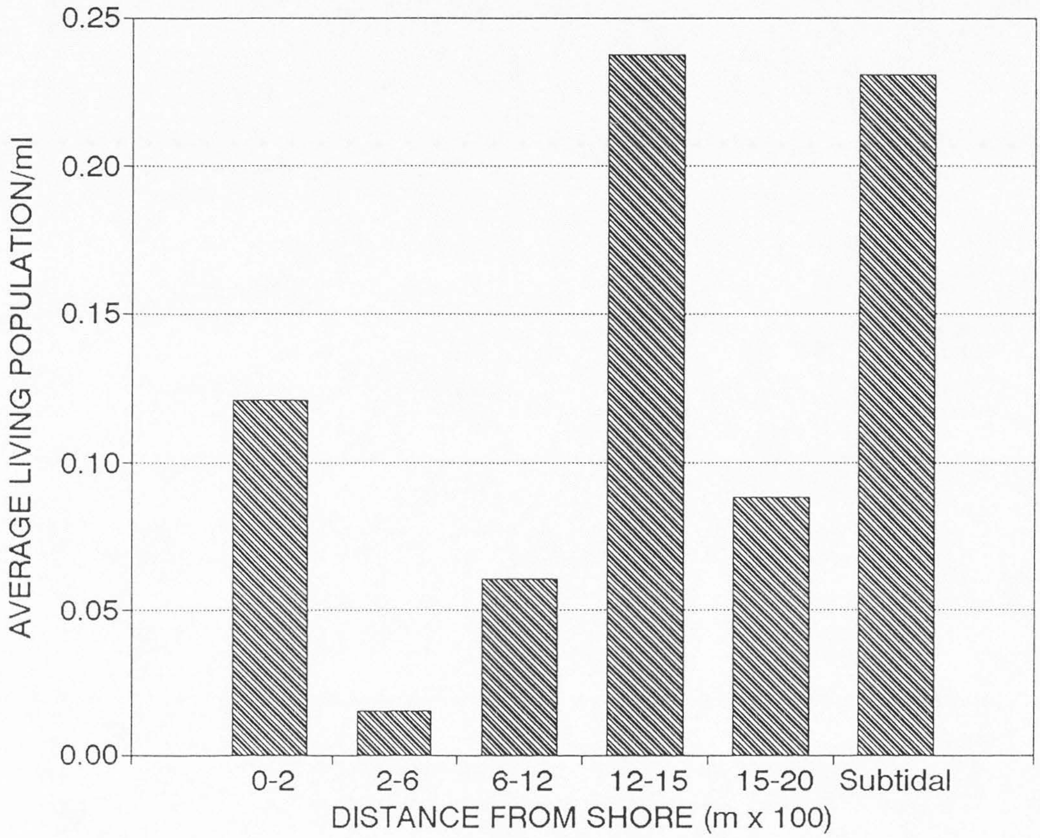

FIGURE 25-Distribution of average living populations (July 1991) of benthonic Foraminifera per ml of sediment from inner flat to subtidal zones in Bahia la Choya.

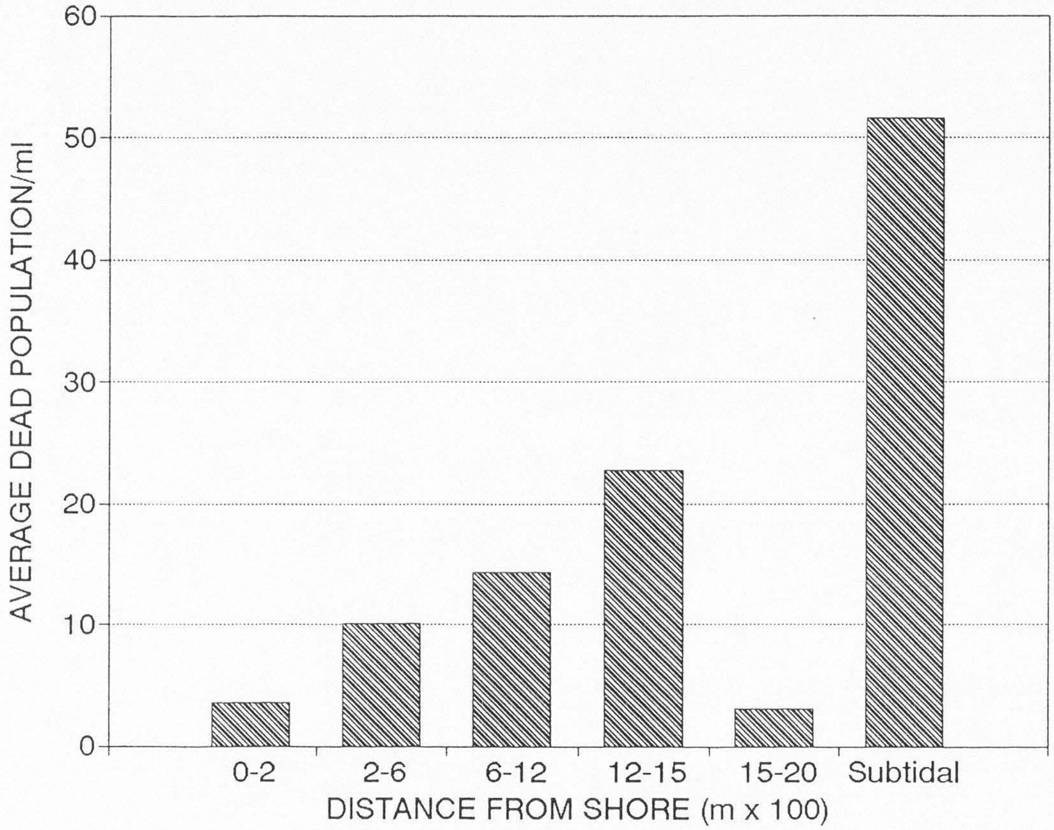

FIGURE 26-Distribution of average dead populations (July 1991) of benthonic Foraminifera per ml of sediment from inner flat to subtidal zones in Bahia la Cholla.

raminifera. The ratios of living to total populations of benthonic Foraminifera are distinctly bimodal. In the 200 - 600 m, 600 - 1200 m, and subtidal zones, the ratios are all less than 1% (Fig. 27). The ratio increases to nearly 3% in the 1200 - 1500 m and 1500 - 2000 m zones, and to 3.61% in the 0 - 200 m zone (Fig. 27).

Bioerosion Intensity

Twenty-one specimens of *Quinqueloculina* sp. (suborder Miliolina) and *Elphidium* sp. (suborder Rotaliina) from various locations were used to examine biological destruction of foraminiferal tests. Miliolina specimens are most characterized by circular holes produced by microborers while Rotaliina specimens are characterized by a combination of holes and filament tracings produced by microborers (Figs. 28 and 29). Table 10 shows total areas and damaged areas of specimens and ratios (%) of damaged areas. The ratios range from 1.1% to 15.8% with an average value of 4.2% ± 2.9 for Miliolina and from 2.1% to 27.7% with an average value of 12.8% ± 6.9 for Rotaliina; these are significantly different (MWU, $p < 0.05$).

Of the ten *in situ* bioerosion experiments, only the one located just outside of CEDO (Centro Intercultural de Estudios de Desiertos y Océanos, A. C.) was retrieved from the field after 6 months (Fig. 7). Examination by Scanning Electron Microscope revealed that the test surfaces of all

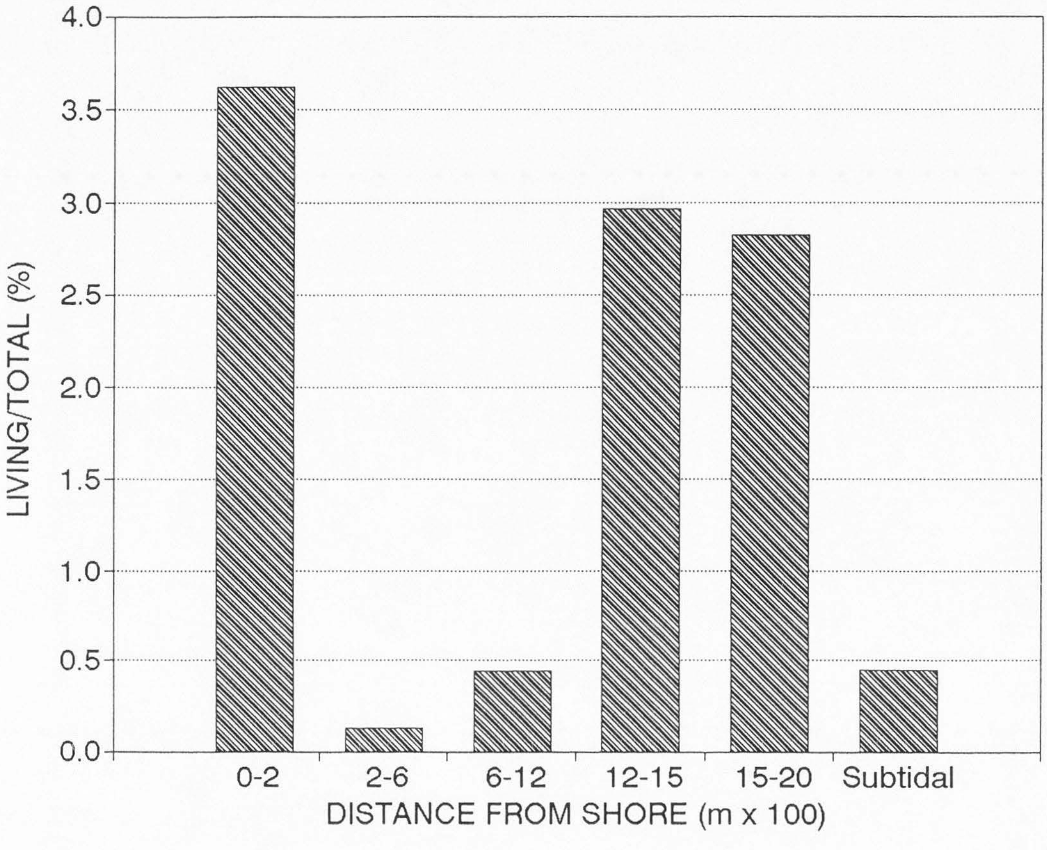

FIGURE 27-Living-total population ratios (July 1991) of benthonic Foraminifera from inner flat to subtidal zones in Bahia la Cholla.

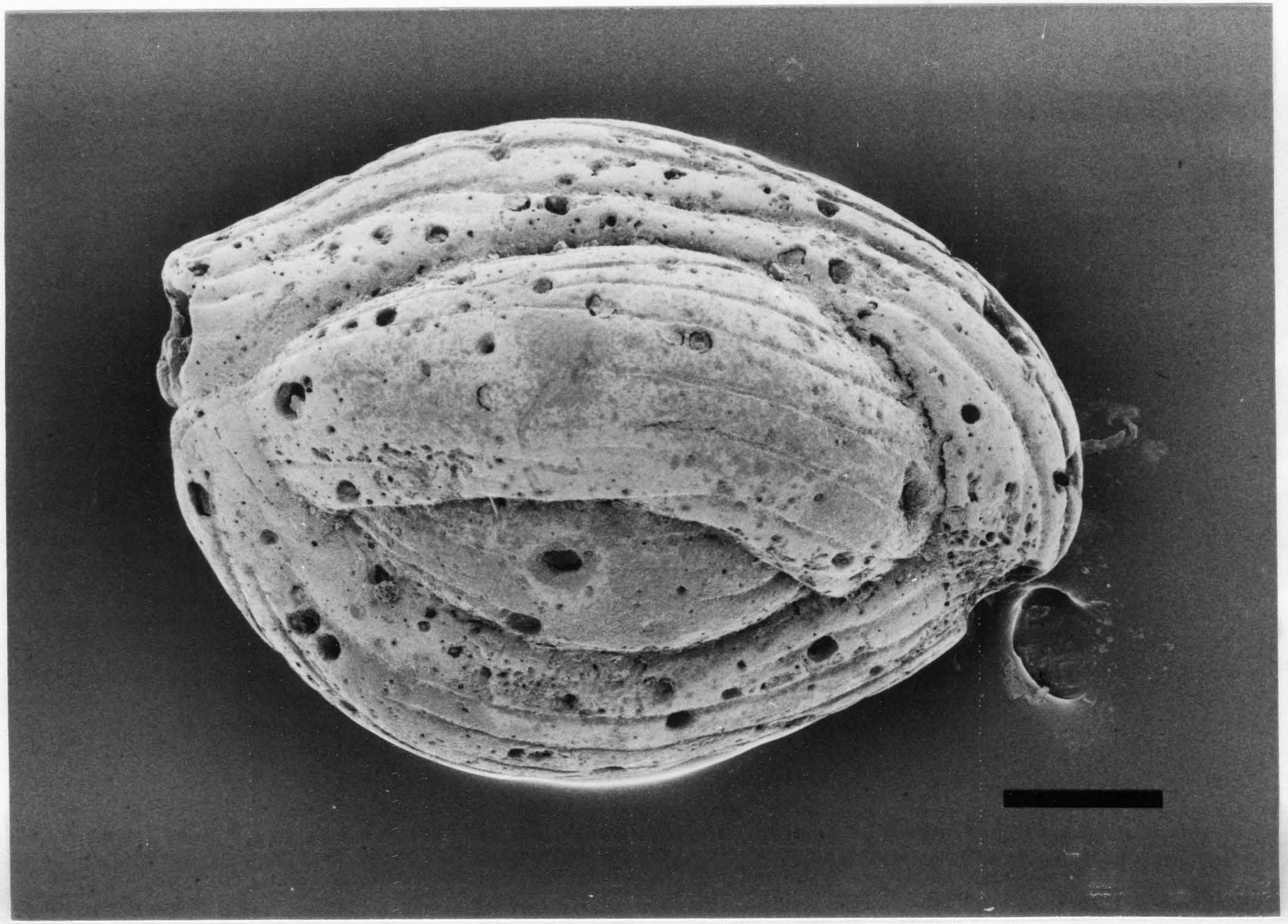

FIGURE 28-Miliolina specimen (*Quinqueloculina seminulum*) which shows circular holes produced by microborers. The scale bar represents 100 μm.

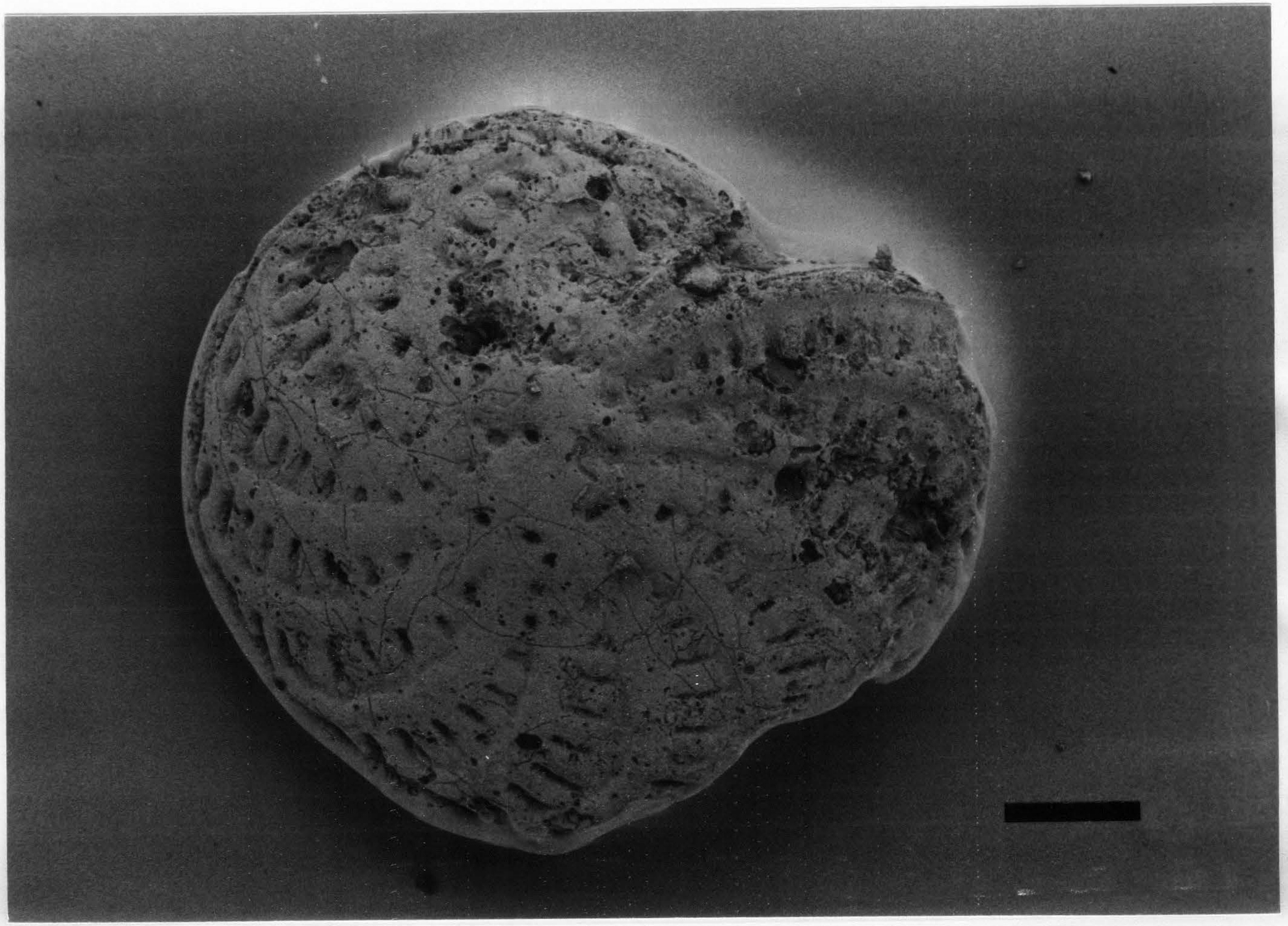

FIGURE 29-Rotaliina specimen (*Elphidium* cf. *E. crispum*) which shows a combination of holes and filament tracings produced by microborers. The scale bar represents 100 μm.

TABLE 10-Damaged/whole area ratios of bioeroded Foraminifera tests.

Sample #	Traverse #	Distance[a] (m)	Total Area (mm^2)	Damaged Area (mm^2)	Ratio (%)
Suborder Miliolina					
1-1	IV	Subtidal	0.0472	0.0010	2.1
1-2	I	1800	0.0526	0.0083	15.8
9-1	V	134	0.0335	0.0009	2.7
9-2	IV	100	0.0350	0.0004	1.1
9-3	III	300	0.0930	0.0022	2.4
9-4	IV	134	0.0475	0.0006	1.3
10-1	V	Subtidal	0.0581	0.0026	4.5
10-2	I	Subtidal	0.0444	0.0032	7.2
10-3	III	100	0.0478	0.0014	2.9
11-1	III	100	0.0781	0.0017	2.2
11-2	III	Subtidal	0.0759	0.0028	3.7
				Mean	4.2
				95% C.I.	±2.9
Suborder Rotaliina					
3-1	III	100	0.0759	0.0018	2.4
3-3	I	1700	0.0455	0.0036	7.9
4-1	V	Subtidal	0.0828	0.0219	26.4
4-4	III	200	0.0974	0.0270	27.7
5-4	I	1700	0.0373	0.0008	2.1
8-1	III	Subtidal	0.1172	0.0254	21.7
8-2	IV	402	0.1221	0.0163	13.3
8-3	II	Subtidal	0.1368	0.0213	15.6
8-4	V	200	0.0437	0.0024	5.5
10-4	I	1800	0.1041	0.0055	5.3
				Mean	12.8
				95% C.I.	±6.9

[a] Distance seaward from the shore.

the specimens on that stake were completely destroyed (Figs. 30 and 31). This may reflect a combination of bioerosion, dissolution, and abrasion.

Transport Potential

Settling Velocities

Results of the measurements of settling velocities for five of the most common species are summarized in Table 11. All the values are averages of each parameter for each species. The range of settling velocities is 0.8 to 4.5 cm/sec for the taxa studied. The settling motions of the specimens involved in the experiments were mainly straight falling, occasionally with a slight oscillating motion in *Elphidium* cf. *E. gunteri* and in *Elphidium articulatum* var. *rugulosum*. Evaluation of the accuracy of the mean settling velocities based on five replicates for each specimen shows that 86 of 93 settling-velocity means (92%) have ± 6% precision at a 95% confidence level.

The settling velocities were tested regressively against the various test parameters (Table 1). Six of the 13 independent variables have significant regressive relationships with settling velocity. These are, in descending order of importance, weight (log - log) (r = 0.9562), nominal diameter (r = 0.8853), volume (r = 0.8813), the shortest intercept (r = 0.8594), the intermediate intercept (r = 0.8509), and the

FIGURE 30-Miliolina specimen (*Quinqueloculina tricarinata*) exposed to bioeroders for a six-month interval. The test surface was completely destroyed. The scale bar represents 400 μm.

FIGURE 31-Rotaliina specimen (*Discorbis rosea*) exposed to bioeroders for a six-month interval. The test surface was completely destroyed. The scale bar represents 100 μm.

TABLE 11-The mean settling and movement-threshold velocities for Foraminifera species with relevant test parameters, as well as their 95% confidence intervals (see Table 1 for definitions of test parameters).

Species	SetVel[a] (cm/sec)	T (F)[b] (cm/sec)	T (C)[c] (cm/sec)	Ds (mm)	Di (mm)	Dl (mm)	Weight (mg)	Volume (mm^3)	Porosity	DWAT[d] (mg/mm^3)	Ds/Di	Di/Dl	CSF	Dn (mm)	MPS	OS	SHAPE
Buccella mansfieldi	1.9 ±0.2 (21)[e]	2.4 ±1.5 (10)	12.6 ±3.4 (10)	0.26 ±0.01 (21)	0.38 ±0.02 (21)	0.44 ±0.02 (21)	0.015 ±0.003 (21)	0.023 ±0.003 (21)	0.75 ±0.04 (21)	1.42 ±0.08 (21)	0.69 ±0.03 (21)	0.86 ±0.02 (21)	0.64 ±0.03 (21)	0.35 ±0.02 (21)	0.74 ±0.02 (21)	0.80 ±0.02 (21)	Ellipsoid
Elphidium articulatum var. *E. rugulosum*	1.3 ±0.1 (18)	6.1 ±4.5 (7)	14.1 ±6.4 (7)	0.18 ±0.01 (18)	0.32 ±0.02 (18)	0.39 ±0.03 (18)	0.009 ±0.002 (18)	0.013 ±0.003 (18)	0.71 ±0.04 (18)	1.49 ±0.08 (18)	0.56 ±0.02 (18)	0.83 ±0.02 (18)	0.51 ±0.02 (18)	0.28 ±0.02 (18)	0.64 ±0.02 (18)	0.73 ±0.02 (18)	Disc
Elphidium cf. *E. crispum*	3.1 ±0.4 (15)	3.9 ±2.2 (8)	10.5 ±3.5 (8)	0.31 ±0.03 (15)	0.53 ±0.05 (15)	0.60 ±0.05 (15)	0.056 ±0.016 (15)	0.056 ±0.016 (15)	0.63 ±0.03 (15)	1.63 ±0.05 (15)	0.59 ±0.02 (15)	0.87 ±0.01 (15)	0.55 ±0.01 (15)	0.46 ±0.04 (15)	0.67 ±0.01 (15)	0.77 ±0.01 (15)	Disc
Elphidium cf. *E. gunteri*	1.8 ±0.2 (19)	6.7 ±5.5 (6)	8.6 ±2.6 (5)	0.21 ±0.01 (19)	0.34 ±0.03 (19)	0.40 ±0.03 (19)	0.015 ±0.004 (19)	0.016 ±0.003 (19)	0.66 ±0.04 (19)	1.58 ±0.06 (19)	0.63 ±0.03 (19)	0.85 ±0.02 (19)	0.60 ±0.05 (19)	0.30 ±0.01 (19)	0.69 ±0.02 (19)	0.77 ±0.02 (19)	Disc
Quinqueloculina seminulum	1.8 ±0.1 (20)	2.5 ±1.2 (13)	9.7 ±3.7 (13)	0.24 ±0.02 (20)	0.32 ±0.03 (20)	0.50 ±0.04 (20)	0.017 ±0.002 (20)	0.021 ±0.005 (20)	0.67 ±0.03 (20)	1.56 ±0.05 (20)	0.75 ±0.02 (20)	0.65 ±0.05 (20)	0.60 ±0.03 (20)	0.33 ±0.02 (20)	0.71 ±0.02 (20)	0.68 ±0.03 (20)	Ellipsoid

[a] SetVel refers to settling velocity.
[b] T (F) refers to threshold velocity with a fixed fine-sand platform.
[c] T (C) refers to threshold velocity with a fixed coarse-sand platform.
[d] DWAT refers to effective density in water.
[e] The numbers in parentheses represent the numbers of individual tests used.

longest intercept ($r = 0.8015$) (Fig. 32). Further examination by step-wise multiple-regression analysis revealed that six independent variables have significant correlations to the settling velocity with a R-squared value of 0.9509. These include weight, the shortest intercept, effective density in water, maximum projection sphericity, volume, and Corey Shape Factor. Again, the multiple-regression analysis indicates that weight plays the most important role in the regression equation, and accounts for 87.74% of the variance in values of settling velocities, while the combination of the remaining five independent variables only accounts for an additional 7.35% of the variance in values of settling velocities. Apparently the weight of the foraminiferal test is the most important measured attribute in describing the settling velocity. Because weight is not a good measure for fossils, but does have a significant regressive relationship with the nominal diameter ($r = 0.8857$)(Fig. 33), the latter is, therefore, preferred here as a useful parameter and was used in the final multiple-regression analysis. The result of this analysis, using both robust-regression and stepwise-regression techniques, provides a simple predictive equation for settling velocity with a correlation coefficient value of 0.9354, being written as follows:

$$Y = 7.89\ X - 0.76 \qquad (1)$$

where Y is the settling velocity, X is the nominal diameter of the foraminiferal test, and -0.76 is the intercept of the

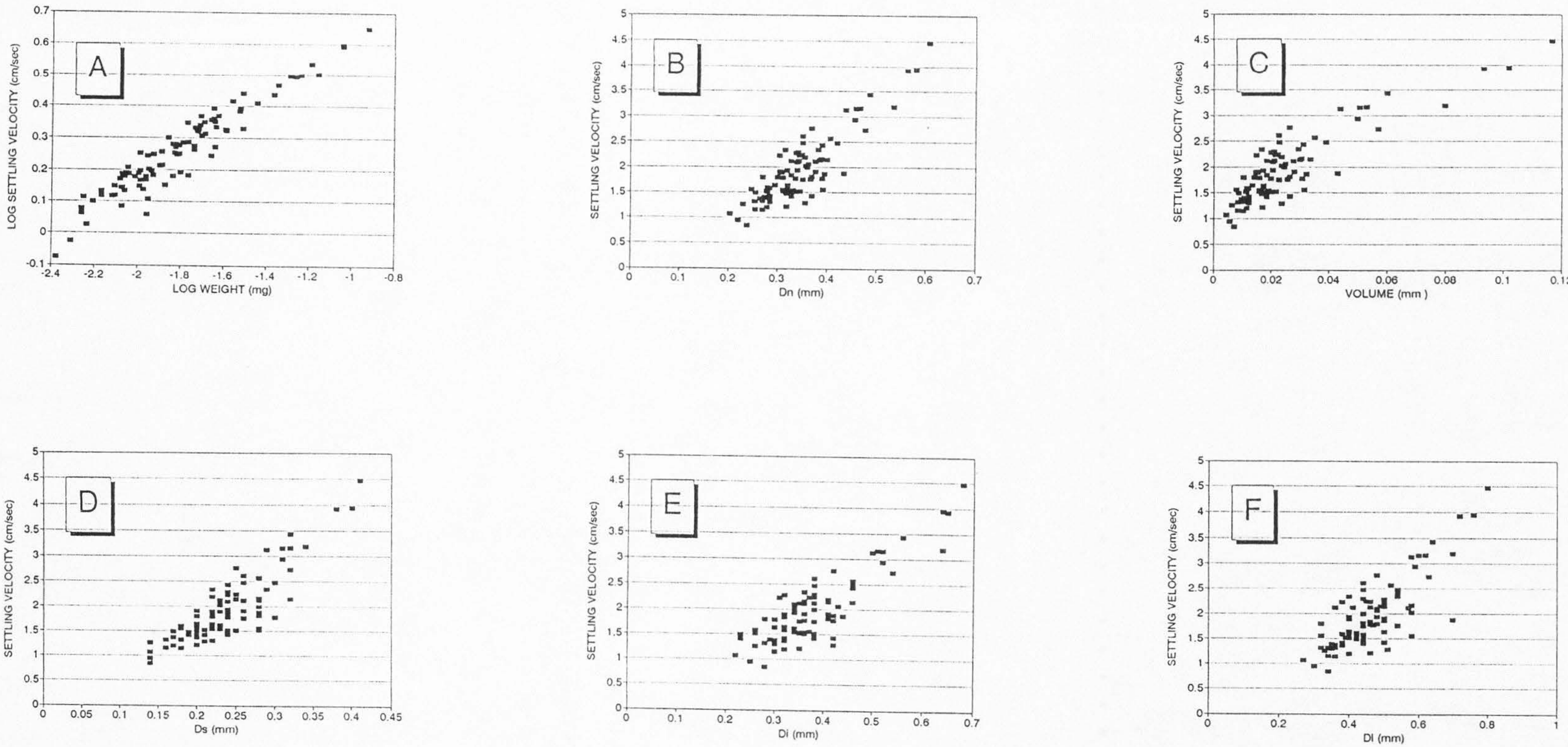

FIGURE 32-Settling velocity versus (A) weight (log - log), (B) nominal diameter, (C) volume, (D) the shortest intercept, (E) the intermediate intercept, and (F) the longest intercept.

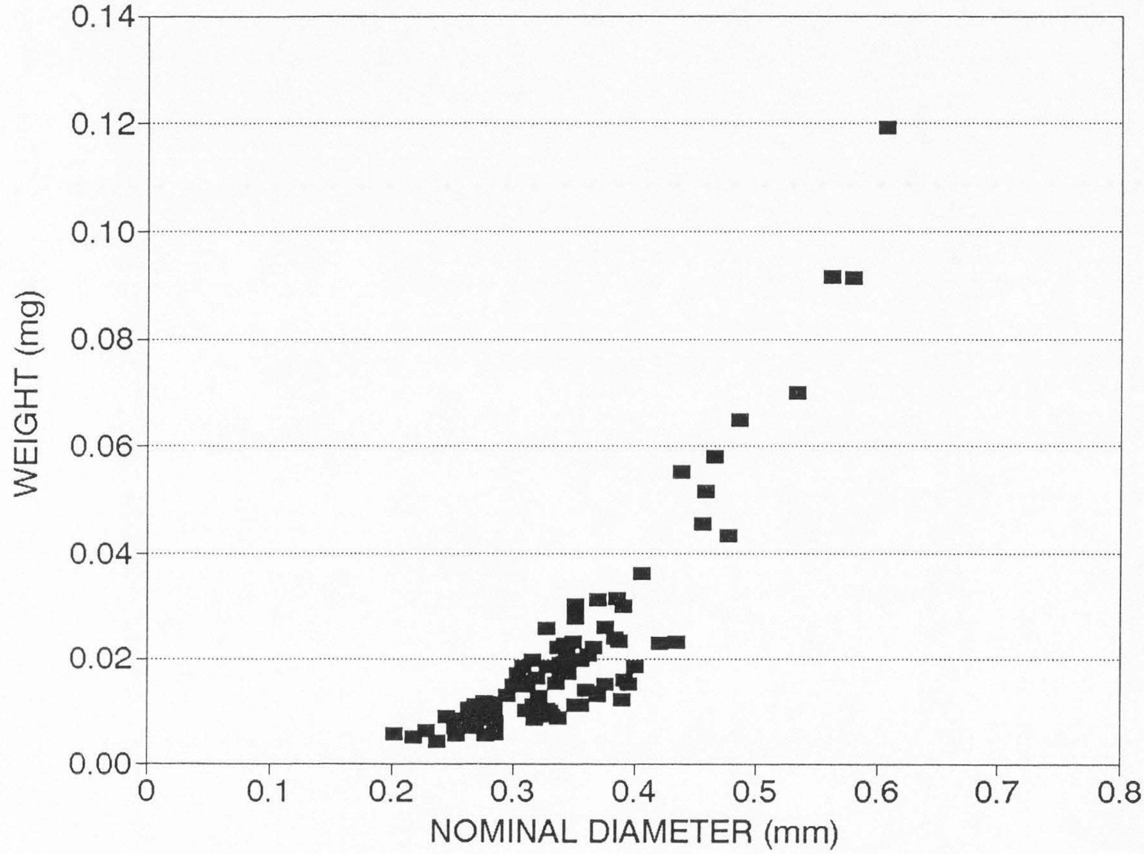

FIGURE 33-Weight versus nominal diameter (D_n).

regression line. Table 12 lists average values of the observed and predicted settling velocities, as well as their residuals, based on the predictive equation for the five studied species.

Movement-Threshold Velocities

The average movement-threshold velocities for the studied species vary from 2.4 cm/sec for *Buccella mansfieldi* on the fixed fine-sand platform to 14.1 cm/sec for *Elphidium articulatum* var. *rugulosum* on the fixed coarse-sand platform (Table 11). The drastic change of the threshold velocities with the different natures of the substrate shows that the sizes of foraminiferal tests and the grain sizes of substrate are two major factors which determine the ease of initial movement of Foraminifera by unidirectional currents. The results indicate that the smaller sizes of foraminiferal tests have higher threshold velocities on the larger-grain-size substrates. The types of initial movement of foraminiferal tests mainly depend on the grain size of the substrate, and vary from rolling and sliding transport, observed predominantly when using the fine-sand platform, to saltation and suspension transport, observed predominantly when using the coarse-sand platform (Table 13).

Statistical analyses reveal some relationships between threshold velocity and other parameters, but no single parameter can predict the threshold velocity. Multiple-regres-

TABLE 12-Observed and predicted average settling velocities (cm/sec) and their residuals for five Foraminifera species using equation (1).

Species	Observed	Predicted	Residuals
Buccella mansfieldi	1.868	1.990	0.122
Elphidium articulatum var. *E. rugulosum*	1.294	1.474	0.180
Elphidium cf. *E. crispum*	3.056	2.891	0.165
Elphidium cf. *E. gunteri*	1.798	1.642	0.156
Quinqueloculina seminulum	1.840	1.873	0.033

TABLE 13-Frequency of occurrence of initial movement types of foraminiferal tests with fine-sand and coarse-sand substrates.

Species	# Individuals of Initial Movement Types (fine-sand substrate)				# Individuals of Initial Movement Types (coarse-sand substrate)				
	Rolling	Sliding	Saltation	Suspension	Rolling	Sliding	Flipped	Saltation	Suspension
Buccella mansfieldi	6	3	1					2	8
Elphidium articulatum var. *E. rugulosum*	1	4		2					7
Elphidium cf. *E. crispum*	4	4			1			7	
Elphidium cf. *E. gunteri*		4		2				5	
Quinqueloculina seminulum	4	8	1			2	1	3	7
Total #	15	23	2	4	1	2	1	17	22

sion analyses using robust- and stepwise-regression techniques provide two predictive equations for movement-threshold velocities:

$$Y_1 = 32.41X_1 - 56.38X_2 + 23.5 \quad (2)$$

where Y_1 is the threshold velocity with a fixed fine-sand platform, X_1 is the Corey Shape Factor, X_2 is the maximum projection sphericity, and 23.5 is the intercept of the regression plane; and

$$Y_2 = 33.08X_3 - 50.38X_4 - 14.87X_5 + 45.83 \quad (3)$$

where Y_2 is the threshold velocity with a fixed coarse-sand platform, X_3 is the minimum intercept of the foraminiferal test, X_4 is the maximum intercept of foraminiferal test, X_5 is the effective density in water of a foraminiferal test, and 45.83 is the intercept of the regression plane. Multiple correlation coefficient values for each equation are 0.7142 and 0.6786, respectively. Tables 14 and 15 list average values of the observed and predicted threshold velocities, as well as their residuals, based on the predictive equations for the five species studied.

TABLE 14-Observed and predicted average threshold velocities (cm/sec) and their residuals with a fixed fine-sand substrate for five Foraminifera species using equation (2).

Species	Observed	Predicted	Residuals
Buccella mansfieldi	2.400	2.174	0.226
Elphidium articulatum var. *E. rugulosum*	6.143	3.915	2.228
Elphidium cf. *E. crispum*	3.875	3.356	0.519
Elphidium cf. *E. gunteri*	6.667	5.232	1.435
Quinqueloculina seminulum	2.462	2.669	0.207

TABLE 15-Observed and predicted average threshold velocities (cm/sec) and their residuals with a fixed coarse-sand substrate for five Foraminifera species using equation (3).

Species	Observed	Predicted	Residuals
Buccella mansfieldi	12.600	13.170	0.570
Elphidium articulatum var. *E. rugulosum*	14.143	14.659	0.516
Elphidium cf. *E. crispum*	10.500	8.850	1.650
Elphidium cf. *E. gunteri*	8.600	10.676	2.076
Quinqueloculina seminulum	9.692	8.120	1.572

DISCUSSION

Insoluble-Residue Content

A notable decrease in percent total insoluble-residue content is observed between the intertidal and subtidal zones while changes of percent total insoluble residue content within the intertidal zone are generally not significant. The sediment insoluble-residue content has the highest value in the inner-flat zone, gradually decreases towards the middle- and outer-flat zones, and has the lowest values in the subtidal zone, except for a narrow belt near the shore and the Traverse I channel area, which have sightly lower total insoluble residue contents. The subtidal zone, with abundant rocky substrates, may be an ideal place for many different species because of its irregular topography and intermixed patches of sand, thus resulting in high rates of shell production (Meldahl, 1990). Meldahl (1990) also described the effects of longshore movement, which may be responsible for the high shell concentrations along the beach at Bahia la Choya. The perennial flooding and significant transport along the tidal channel are likely causes for shell concentrations there. The variation in total insoluble-residue content of Traverses V and VI results from the irregular topography of rocky substrates, where relatively more shell materials are concentrated in lower-topography depressions formed adjacent to nearby rocky substrates (Fig. 11). The differences in total insoluble-residue contents among channel, intertidal, and subtidal sediment samples are also shown by Q-mode cluster analysis with three well-defined associations (with only a few exceptions)(Fig. 13). Within the intertidal group, Traverse VI samples are separated from the others.

Constituent-Particle Composition

The relatively low number of grain types (12) in the Holocene sediment samples resulted in relatively low counts (300-400) required to reach the flattening of the cumulative rarefaction curves. Quartz and unidentified molluscan shell fragments are the two dominant constituent particles in sediment, and, together, account for more than 85% of the total constituents. They also exhibit significant zonation differences when their percent composition in sediment is plotted against distance from the shore (Fig. 34). Quartz in the sediment is very abundant throughout the intertidal zone, averaging from 75.9% to 85.1%, but shows a striking decline in abundance in sediments of the subtidal zone, averaging down to only 29.7% (Fig. 34). By comparison, unidentified molluscan shell fragments exhibit an opposite trend, being much more abundant in sediment in the subtidal zone (average 49.0%) than in the intertidal zone (average 5.4% - 16.3%) (Fig. 34). Therefore, an increase in shell production from the inner flat to subtidal zones overwhelms the supply of

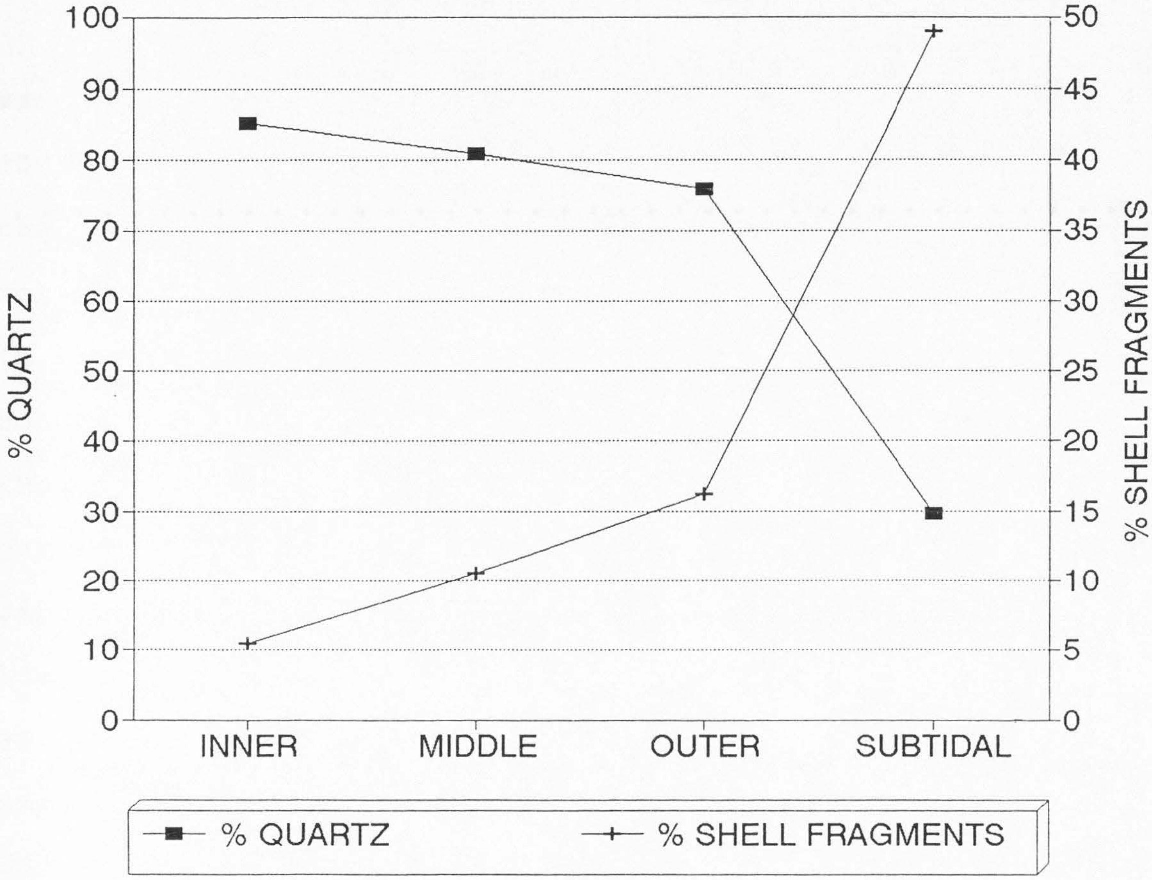

FIGURE 34-Percent compositions of quartz and unidentified molluscan shell fragments in sediments, which show differences between intertidal and subtidal areas (Table 4). Inner, middle, outer, and subtidal zones represent 0 - 600 m, 600 - 1200 m, 1200 - 2500 m, and > 2500 m seaward zones, respectively.

quartz sand. This is also reflected in the distribution of carbonate/noncarbonate ratios. The dendrogram obtained from Q-mode cluster analysis further reveals four distinctive groupings representing inner flat, middle flat, outer flat, and subtidal facies, respectively (Fig. 15).

Low constituent-particle diversity in Pleistocene rock samples also results in low thin-section point-counts (300-400) required to flatten the rarefaction curves. Along with the fine-grained carbonate matrix, quartz and unidentified molluscan shell fragments are again the dominant components in the rock samples. In addition, some of the Pleistocene rock may have been reworked into the Holocene sediments (Ronald E. Martin, personal communication). The component percentages of the rock samples indicate that the Pleistocene marine deposits probably represent a low intertidal or shallow subtidal zone, deposited during a highstand of sea level at approximately 120 ka (Ortlieb, 1981). Q-mode cluster analysis of constituent-particle data (Table 5) shows that two groups are present among samples from the Pleistocene outcrops (Fig. 16). The difference between the two groups may result from different biotic communities, which represent different depositional environments.

Texture

The statistical parameters of texture also emphasize the difference between intertidal and subtidal sediment samples.

The intertidal sediment has a finer mean grain size (M_z = 2.73 ± 0.15), is moderately well sorted (IGSD = 0.65 ± 0.09), and is coarse skewed (SK_i = -0.19 ± 0.07). On the other hand, the subtidal sediment has a medium mean grain size (M_z = 1.41 ± 0.33), is poorly sorted (IGSD = 1.30 ± 0.19), and is near symmetrically skewed (SK_i -0.07 ± 0.10). In addition, mean grain size (M_z) shows a significant negative correlation to depth, especially within Traverses I - V (Fig. 20). Plots of median grain size (M_d) and mean grain size (M_z) against sorting (IGSD) and skewness (SK_i) all show that two different groups, representing intertidal and subtidal sediment samples, are present in the study area (Fig. 22). The reasons for this characteristic distribution of sediment in intertidal and subtidal zones probably are due partly to higher energy levels and partly to the transport mechanisms involved. The wave and current energy is generally stronger in the lower part of the intertidal zone and in the subtidal zone than in the upper part of the intertidal zone. Thus, coarser sediment is relatively enriched on the topographically lower part of the tidal flats, whereas finer sediment is relatively concentrated on the topographically higher part of the tidal flats. In addition, bidirectional transport by currents of unequal velocity can produce the same distribution because the current velocity needed to erode the sediment of a given size (ebb-current velocity) is much higher than the velocity needed to deposit it (flood-current velocity)(Hjulström's diagram, Sundborg, 1956). Sumpter (1987) pointed out that the majority of nonbiogenic sediment in the study area came from Punta Pelicano, which is a granitic highland on the south side of Bahia la Choya (Fig. 1). The northward increase in sediment sorting and decrease in mean grain size supports Sumpter's conclusion, because poorly or moderately sorted sediment with a finer mean grain size is more likely to occur near the source rock, whereas moderately well- or well-sorted sediment with a coarser mean grain size is more likely to occur farther from the source rock.

Q-mode cluster analysis of sediment textural values results in two major groupings representing intertidal and subtidal zones, and two subgroupings within the intertidal zone (Fig. 23). The S-N zonation within the intertidal grouping further supports the conclusion about the sediment sources in the study area.

Distribution of Living and Dead Benthonic Foraminifera

The purpose of the distribution studies of benthonic Foraminifera was to determine an approximation of relative sedimentation rates and/or rates of test destruction by taphonomic processes in the study area by calculating the ratios of live to total benthonic Foraminifera. Previous studies by Walton (1955) and Phleger (1960) showed that lower living-total ratios could indicate relatively slow sedimentation, which meant that a large population of dead Foraminifera accumulated, and that higher living-total ratios could indicate relatively rapid sedimentation, which meant that a small population of dead Foraminifera accumulated.

This study indicated that very small living populations (less than 1/ml) are present in the study area. The much greater dead population per milliliter and total population per milliliter, therefore, are nearly the same, and gradually increase from 0 - 200 m to the subtidal zones, except for a decrease at the 1500 - 2000-m seaward zone. This is most likely due to the fact that the more offshore environments are better habitats for Foraminifera, as they suffer less exposure during the tidal cycle (Fig. 26). The reason why dead populations per milliliter in the 1500 - 2000-m seaward zone have very low values is unclear. A possible explanation is that in this lower part of the intertidal zone the wave and current energy is generally stronger, and, thus, plays an important role in destroying foraminiferal tests. Flessa et al. (1993) indicated that the taphonomic condition of shells in Bahia la Choya was more likely the result of their total residence time on the surface of sediments than its time-since-death (surface time plus burial time). The relatively stronger energy at the 1500 - 2000-m zone could increase residence time of foraminiferal tests on the surface so as to result in more tests destroyed. The living-total ratios are all low, being less than 1% in 200 - 600-m, 600 - 1200-m, and subtidal zones, and being over 2.5% in 0 - 200-m, 1200 - 1500-m, and 1500 - 2000-m zones (Fig. 27). The results apparently show that the study area is located in a relatively low sedimentation environment, which is consistent with the conclusions of Flessa and Ekdale (1987) and Flessa et al. (1993). Higher living-total ratios at 0 - 200-m, 1200 - 1500-m, and 1500 - 2000-m seaward zones may be due to tests of the living Foraminifera not being diluted by large numbers of tests of the dead Foraminifera. In addition, the number of total Foraminifera shows significant correlation to percent calcium carbonate (SRC, $p < 0.05$)(Fig. 35). The relationship may indicate that higher $CaCO_3$ content (shells) acts as a buffer and protects foraminiferal tests from dissolution by undersaturated poor water (Martin, 1993).

Bioerosion Intensity

Differences exist at the subordinal level in both types and degrees of bioerosion. In the two genera used in this study (*Quinqueloculina* and *Elphidium*), the greater number of surface openings of *Elphidium* specimens is likely to provide ideal places for microborer dwelling, and, therefore, result in multi-bioerosion types and higher ratios of damaged areas on foraminiferal tests (Figs. 28 and 29, Table 10). The results do not parallel the findings of Peebles and Lewis (1988), and Martin and Liddell (1991), who found a greater frequency/intensity of microboring in tests of miliolinid

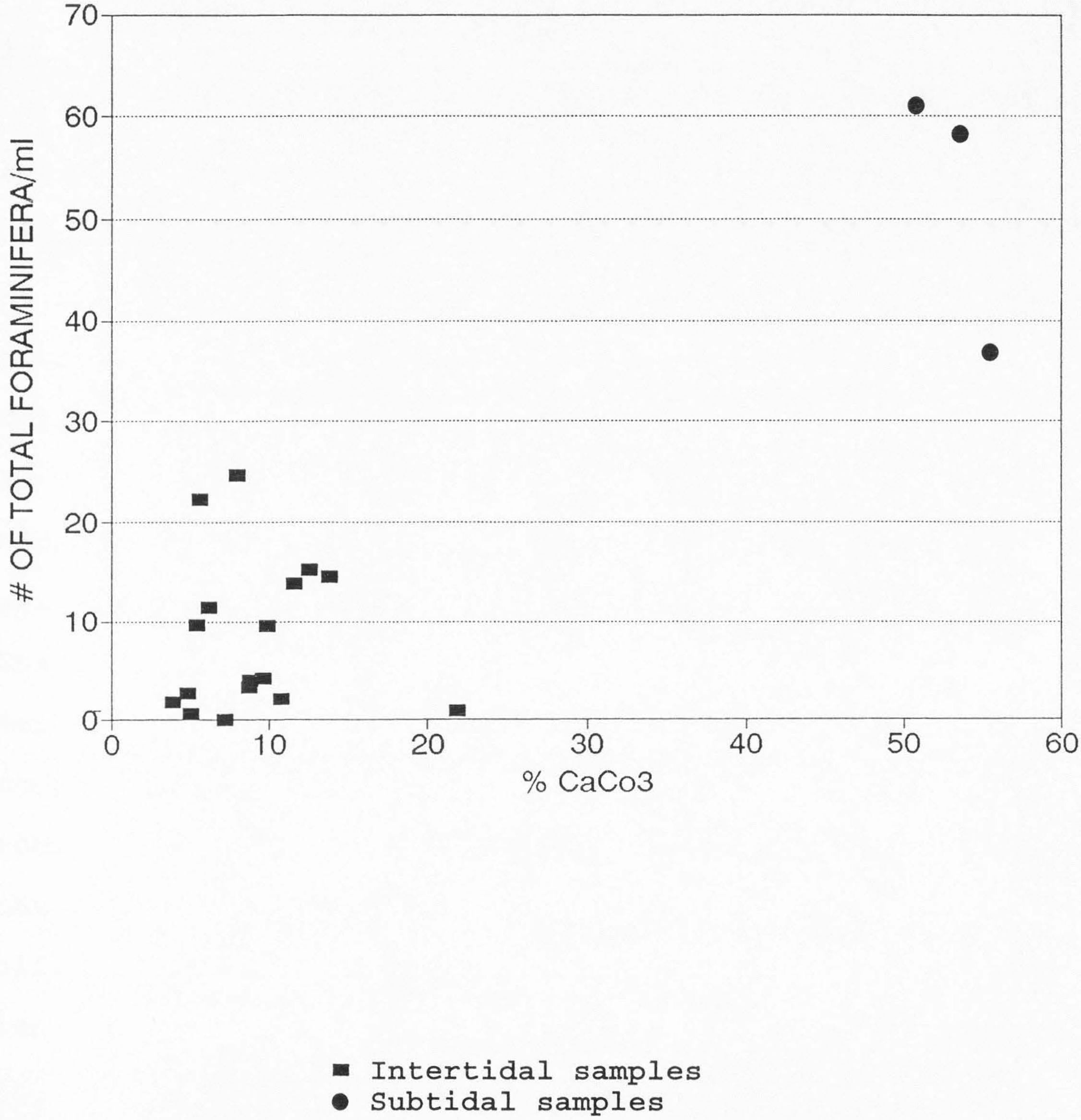

FIGURE 35-Plot of number of total Foraminifera/ml versus percent calcium carbonate for samples from Bahia la Choya, Mexico.

than of rotalinid Foraminifera in carbonate environments. Peebles and Lewis (1988), however, also indicated that the degree of microboring in *Quinqueloculina* tests is often slight. Thus, differences in susceptibility to bioerosion exist not only at the subordinal level but also at the generic level.

The rapid destruction of specimens in the *in situ* bioerosion experiments in this study may be the result of corrasion by biological, chemical, and physical processes. Martin et al. (1992) have indicated that both abrasion and dissolution are strong in Bahia la Choya, although which action is dominant during the degradation process of tests is unclear. In other studies at Discovery Bay, Jamaica (Martin and Liddell, 1991), similar *in situ* bioerosion experiments were performed, and the intensity of bioerosion was remarkable. Specimens of *Archaias angulatus* (suborder Miliolina) and *Amphistegina gibbosa* (suborder Rotaliina) were nearly or completely destroyed by bioerosion in those carbonate environments over a 3-month interval. Both experimental studies, thus, revealed that bioerosion had strong effects on foraminiferal test destruction in siliciclastic and carbonate environments.

Transport Potential

Settling Velocities

The repeatability of the measured settling rates of foraminiferal tests assessed in this study gave a slightly higher error percentage than the results of Gibbs et al. (1971), about 4% at a 95% confidence level. The poorest precision among all the repeated settling measurements is that for *Elphidium articulatum* var. *rugulosum*, the smallest and lightest species in this study, which may reflect trapped air in the tests, despite vacuum immersion of tests in water prior to experimentation. In addition, higher error percentages are probably due to the diversity of densities and shapes of the Foraminifera. In the study of Gibbs et al. (1971), solid glass spheres were used to evaluate the level of accuracy for the measured settlings. The difference between glass spheres and foraminiferal tests is obvious, as the latter have lower density with empty chambers and non-spherical shapes.

The results of the settling-velocity experiments show that the most important factors influencing the settling velocities of Foraminifera are test size and weight (Table 11, Figs. 32 and 36). Weight, in turn, is related to density. Shape does not appear to be an important factor to influence settling velocity or motion in this study, which is probably due to the relatively small size of the experimental

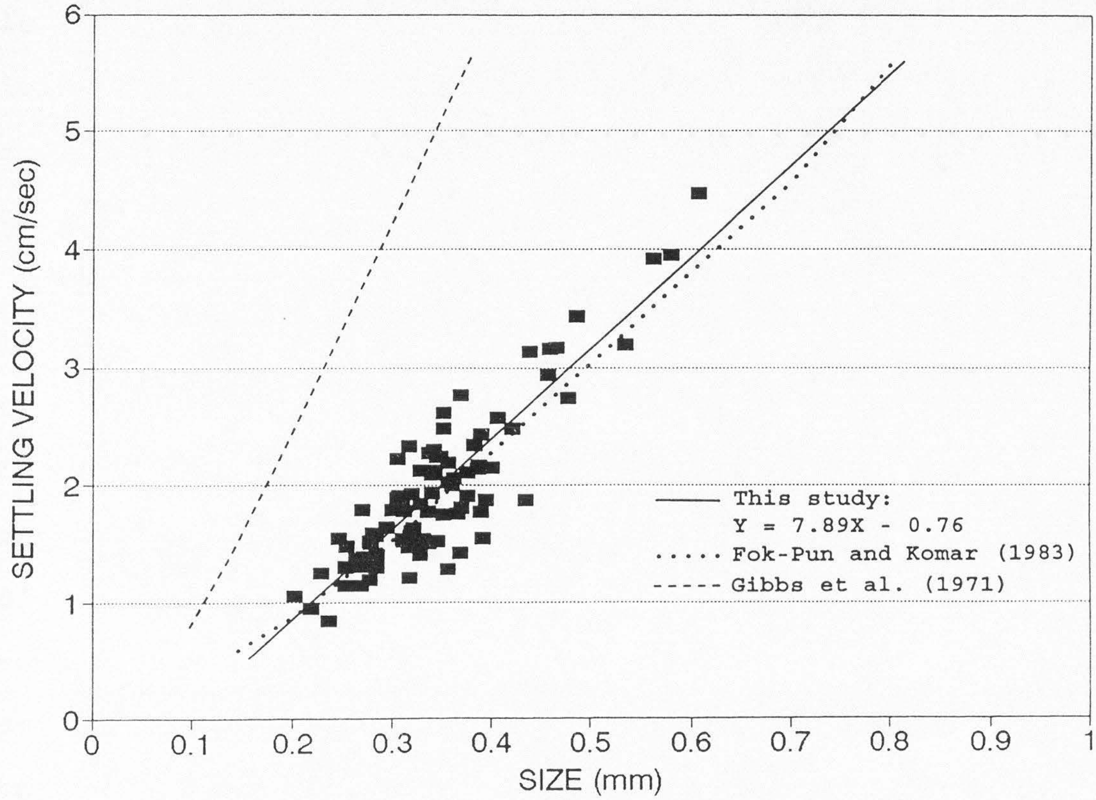

FIGURE 36-Settling velocity versus size with lines calculated by Gibbs et al. (diameter, 1971), Fok-Pun and Komar (diameter, 1983), and proposed equation (1) from this study (nominal diameter, D_n).

taxa. In other studies involving taxa from carbonate environments (e.g., Cunningham et al., 1989; Liddell et al., 1990; Martin and Liddell, 1991), the shapes of Foraminifera did have an effect on settling motion, because of the larger sizes of the experimental taxa and greater diversity of test shapes. In Figure 36, the measured settling velocities are plotted versus size for the five species studied. In addition, a line based on the values for the spherical planktonic Foraminifera, *Orbulina universa*, calculated by Fok-Pun and Komar (1983), and a line based on the values for spheres with a density of 2.65 given by Gibbs et al. (1971), are also plotted. The present data plot well below the line by Gibbs et al. and around the line by Fok-Pun and Komar. Lower densities and nonspherical shapes of the foraminiferal tests contribute to foraminiferal settling velocities occurring below Gibbs's line. The reason for the scatter of data around the Fok-Pun and Komar line is most likely the different densities and shapes of Foraminifera used in these two studies. The results from this research show a good correlation with previous studies done by Maiklem (1968); Berger and Piper (1972); Fok-Pun and Komar (1983); Cunningham et al. (1989); Liddell et al. (1990); and Martin and Liddell (1991). They all demonstrate the effects of size, density, and shape on settling velocities of bioclastic grains, including planktonic and benthonic Foraminifera.

Movement-Threshold Velocities

The results of the flume experiments are also in accord with previous studies, that is, the ease of initial movement of Foraminifera by unidirectional currents is largely determined by the height which they project above the substrate, which, in turn, is a function of shape, orientation, and overall size of the test and the grain size of the substrate (Kontrovitz et al., 1978, 1979; Cunningham et al., 1989; Liddell et al., 1990; Martin and Liddell, 1991). The test shape and orientation exert strong controls on initial movement type and threshold velocity. For example, a platy (blade or disc) shape (*Elphidium articulatum* var. *rugulosum*) usually has a sliding type of initial movement and a relatively high threshold velocity. In contrast, an elongated (rod or roller) shape (*Quinqueloculina seminulum*) usually has a rolling type of initial movement and a relatively low threshold velocity (Table 13). Although the orientations of long axes of foraminiferal tests that are normal or parallel to current flow should be a key factor in the initial movement types and the threshold velocities, the effect was difficult to observe in this study because of the small sizes of specimens.

Threshold velocities and initial movement types of foraminiferal tests are greatly affected by the nature of the substrate upon which the foraminiferal tests occur. The tests are all larger than fine sand, and, except for certain *Elphidium* cf. *E. crispum,* smaller than coarse sand (Table 11). The results show that tests occurring on substrates with a grain size smaller than that of the tests require relatively low flow velocities for the initiation of movement, usually by rolling or sliding. By comparison, tests occurring on substrates with a grain size equal to or larger than that of the tests require much greater flow velocities for the initiation of movement, usually by saltation or suspension (Table 13).

Statistical analyses reveal that no single variable can well describe the threshold velocities with either substrate type. The threshold velocities are definitely affected by multiple variables; therefore, there are additive effects. Two predictive equations were developed by multiple-regression analyses. The predictive equation (2) for threshold velocities with the fixed fine-sand platform includes two variables (MPS and CSF) which are significantly related to the threshold velocity (r = 0.7142) at the 95% level. The predictive equation developed by Kontrovitz et al. (1978) is:

$$Y_1 = 18.4 - 11.4X_2 - 38.9X_6 \qquad (4)$$

where Y_1 is the threshold velocity with a platform covered with a layer of fixed fine sand which was overlain by loose fine sand, X_2 is the maximum projection sphericity, X_6 is the weight, and 18.4 is the intercept of the regression plane. In the equation, Kontrovitz et al. (1978) used the weight variable instead of the Corey Shape Factor variable used in the present study. Weight, however, would be difficult to apply to the evaluation of possible transport of fossil foraminiferal assemblages. Both equations have the same significant correlation at a high level ($r > 0.7000$). The difference between equations (2) and (4) may reflect differences in experimental designs (i.e., loose versus fixed-sand platforms) or may be due to the fact that the measures of size and shape are unequal statistically between the two groups of Foraminifera (Kontrovitz et al., 1979). The predictive equation (3) developed in this study includes three variables (D_i, D_1, and DWAT), which are also significantly related to the threshold velocity ($r = 0.6786$) at the 95% level for the coarse-sand substrate. The need to employ more variables and the somewhat lower correlation of this equation may result from the instability of the foraminiferal test with the coarser-sand substrate. The two multiple-regression equations could effectively provide means of predicting the threshold velocity of Foraminifera through a range of substrate grain sizes.

The physical and hydraulic characteristics of Foraminifera from siliciclastic settings can also be compared to those from tropical carbonate environments examined previously by Cunningham et al. (1989), Liddell et al. (1990), and Martin and Liddell (1991). Tables 16 and 17 show those characteristics of foraminiferal assemblages from Mexican silici-

TABLE 16-Characteristics of Mexican Foraminifera assemblages.

1) Low species diversity (35 species).
2) Low population sizes.
3) Small test sizes (0.27 - 0.80 mm).
4) Few test shapes.
5) Low test weights (0.004 - 0.119 mg).
6) Low settling velocities (0.8 - 4.5 cm/sec).
7) A narrow range of movement threshold velocities (1.0 - 22.0 cm/sec).

TABLE 17-Characteristics of Jamaican Foraminifera assemblages.

1) High species diversity (over 180 species).
2) Large population sizes.
3) Small to large test sizes (0.24 - 2.66 mm).
4) Many test shapes.
5) Low to high test weights (0.001 - 2.101 mg).
6) Low to high settling velocities (0.9 - 10.0 cm/sec).
7) A wide range of movement threshold velocities (1.0 - 85.0 cm/sec).

clastic settings and Jamaican carbonate environments. Combining current and previous research indicates that Foraminifera from Mexico with low settling velocities (0.8 - 4.5 cm/sec) and a narrow range of movement threshold velocities (1.0 - 22.0 cm/sec) are more likely to be transported by currents than those from Jamaica, which show low to high settling velocities (0.9 - 10.0 cm/sec) and a wide range of movement threshold velocities (1.0 - 85.0 cm/sec). Overall, the entire Mexican assemblage is more likely to be transported than the Jamaican fauna. Within the Jamaican fauna, some taxa are easily transported while others are much less so. Therefore, sorted remnants of tropical carbonate faunas might be expected to occur more commonly than those of siliciclastic faunas.

CONCLUSIONS

Quantitative analyses of Holocene sediments from Bahia la Choya, Mexico provide an important tool in the differentiation of zonations based on mineralogical content, constituent composition, and textural parameters. Textural parameters also contribute to the delineation of the sediment transport history in the study area. Quantitative analyses of Pleistocene rock samples are also useful in defining lithofacies. In addition, quantitative analyses of living/dead rations of benthonic Foraminifera delineate relative rates of sediment deposition.

Determination of bioerosion intensity by experimental and quantitative analyses provides estimations of test destruction rates, and is useful in paleoecologic and taphonomic reconstructions. The experimental determination of transport potentials has enabled the delineation of foraminiferal morphotypes that are most likely to be transported. The physical and hydraulic characteristics of Foraminifera, therefore, provide assistance in modeling the hydraulic regime of different environments. Finally, such information may be utilized to distinguish between autochthonous and allochthonous microfossil assemblages in the stratigraphic record, and to interpret paleoenvironments.

REFERENCES

Behrensmeyer, A.K., and Kidwell, S.M., 1985, Taphonomy's contribution to paleobiology: Paleobiology, v. 11, p. 105-119.

Berger, W.H., and Piper, D.J.W., 1972, Planktonic Foraminifera: Differential settling, dissolution, and redeposition: Limnology and Oceanography, v. 17, p. 275-287.

Blatt, H., Middleton, G.V., and Murray, R., 1980, Origin of Sedimentary Rocks, 2nd ed.: Englewood Cliffs, New Jersey, Prentice-Hall, 782 p.

Boss, S.K., and Liddell, W.D., 1987a, Patterns of constituent composition of Jamaican fringing reef facies: Sedimentology, v. 34, p. 77-87.

Boss, S.K., and Liddell, W.D., 1987b, Back-reef and fore-reef analogs in the Pleistocene of North Jamaica: Implications for facies recognition and sediment flux in fossil reefs: PALAIOS, v. 2, p. 219-228.

Brasier, M.D., 1980, Microfossils: London, George Allen and Unwin, 193 p.

Cunningham, J.L., Liddell, W.D., and Martin, R.E., 1989, Hydraulic properties of Foraminifera: Implications for foraminiferal taphonomy: Geological Society of America Abstracts with Programs, v. 21, p. 46.

Flessa, K.W., Cutler, A.H., and Meldahl, K.H., 1993, Time and taphonomy: Quantitative estimates of time-averaging and stratigraphic disorder in a shallow marine habitat: Paleobiology, v. 19, p. 266-286.

Flessa, K.W., and Ekdale, A.A., 1987, Paleoecology and taphonomy of Recent to Pleistocene intertidal deposits, Gulf of California: In Flessa, K.W., ed., Paleoecology and Taphonomy of Recent to Pleistocene Intertidal Deposits, Gulf of California, Paleontological Society Special Publication No. 2, p. 2-33.

Fok-Pun, L., and Komar, P.D., 1983, Settling velocities of planktonic Foraminifera: Density variations and shape effects: Journal of Foraminiferal Research, v. 13, p. 60-68.

Folk, R.L., 1968, Petrology of Sedimentary Rocks: Austin, Texas, Hemphill, 170 p.

Fürsich, F.T., and Flessa, K.W., 1987, Taphonomy of tidal flat molluscs in the northern Gulf of California: Paleoenvironmental analysis despite the perils of preservation: PALAIOS, v. 2, p. 543-559.

Gibbs, R.J., Matthews, M.D., and Link, D.A., 1971, The relationship between sphere size and settling velocity: Journal of Sedimentary Petrology, v. 41, p. 7-18.

Golubic, S., Campbell, S.E., Drobne, K., Cameron, B., Balsam, W.L., Cimerman, F., and DuBois, L., 1984, Microbial endoliths: A benthic overprint in the sedimentary record and a paleobathymetric cross-reference with Foraminifera: Journal of Paleontology, v. 58, p. 351-361.

Hintze, J.L., 1990, Number Cruncher Statistical System Version 5.03, Installation and Reference Manual: Kaysville, Utah, 442 p.

Ingram, R.L., 1971, Sieve analysis: In Carver, R.E., ed., Procedures in Sedimentary Petrology: New York, John Wiley and Sons, p. 49-67.

Ireland, H.A., 1971, Insoluble residues: In Carver, R.E., ed., Procedures in Sedimentary Petrology: New York, John Wiley and Sons, p. 479-498.

Kloos, D.P., 1982, Destruction of tests of the foraminifer *Sorites orbiculus* by endolithic microorganisms in a lagoon on Curacao (Netherlands Antilles): Geologie en Mijnbouw, v. 61, p. 201-205.

Kontrovitz, M., Kilmartin, K.C., and Snyder, S. W., 1979, Threshold velocities of tests of planktic Foraminifera: Journal of Foraminiferal Research, v. 9, p. 228-232.

Kontrovitz, M., Snyder, S.W., and Brown, R.J., 1978, A flume study of the movement of Foraminifera tests: Palaeogeography, Palaeoclimatology, Palaeoecology, v. 23, p. 141-150.

Kotler, E., Martin, R.E., and Liddell, W.D., 1989, Experimental analysis of abrasion-resistance of modern reef dwelling Foraminifera from Discovery Bay, Jamaica: Geological Society of America Abstracts with Programs, v. 21, p. 46.

Kovach, W.L., 1990, Multi-Variate Statistical Package Plus

Version 2.0, Users' Manual: Aberystwyth, Wales, 45 p.

Krumbein, W.C., 1941, Measurement and geological significance of shape and roundness of sedimentary particles: Journal of Sedimentary Petrology, v. 11, p. 64-72.

Liddell, W.D., Boss, S.K., Nelson, C.V., and Martin, R. E., 1987, Sedimentological and foraminiferal characterization of shelf and slope environments (1-234), north Jamaica: In Curran, H.A., ed., Proceedings of the Third Symposium on the Geology of Bahamas, p. 91-98.

Liddell, W.D., and Martin, R.E., 1989, Taphofacies in modern carbonate environments: Implications for formation of foraminiferal sediment assemblages: 28th International Geological Congress, Washington, DC, Abstracts, v. 2, p. 299.

Liddell, W.D., Martin, R.E., and Stirling, D.H., 1990, Hydraulic properties of Foraminifera from shallow-water tropical environments: Significance for the formation of foraminiferal assemblages: Abstracts - Papers, 13th International Sedimentological Conference, Nottingham, England, p. 311-312.

Maiklem, W.R., 1968, Some hydraulic properties of bioclastic carbonate grains: Sedimentology, v. 10, p. 101-109.

Martin, R.E., 1993, Secular variation in microfossil biomineralization: Clues to the biogeochemical evolution of Phanerozoic oceans: Geological Society of America Abstracts with Programs, v. 25, p. 428.

Martin, R.E., Harris, S., and Liddell, W.D., 1992, Relative rates of foraminiferal test destruction in modern carbonate and siliciclastic regimes: Geological Society of America Abstracts with Programs, v. 24, p. 30.

Martin, R.E., and Liddell, W.D., 1988, Foraminiferal depth zonation on a north coast fringing reef (0-75 m), Discovery Bay, Jamaica: PALAIOS, v. 3, p. 298-314.

Martin, R.E., and Liddell, W.D., 1989, Relation of counting methods to taphonomic gradients and information content of foraminiferal sediment assemblages: Marine Micropaleontology, v. 15, p. 67-89.

Martin, R.E., and Liddell, W.D., 1990, Preservation of foraminiferal assemblages in modern carbonate environments: Constraints on paleobiological interpretation: Abstracts - Papers, 13th International Sedimentological Conference, Nottingham, England, p. 329.

Martin, R.E., and Liddell, W.D., 1991, The taphonomy of Foraminifera in modern carbonate environments: Implications for the formation of foraminiferal assemblages: In Donovan, S.K., ed., The Processes of Fossilization: London, Belhaven Press, p. 170-193.

Meldahl, K.H., 1987a, Biogenic and physical modes of stratification and shell bed formation in the Recent intertidal environments of Bahia la Choya: In Flessa, K.W., ed., Paleoecology and Taphonomy of Recent to Pleistocene Intertidal Deposits, Gulf of California, Paleontological

Society Special Publication No. 2, p. 177-188.

Meldahl, K.H., 1987b, Origin of shell beds and evolution of a shelly sand spit, Bahia la Choya, northern Gulf of California: In Flessa, K.W., ed., Paleoecology and Taphonomy of Recent to Pleistocene Intertidal Deposits, Gulf of California, Paleontological Society Special Publication No. 2, p. 189-199.

Meldahl, K.H., 1990, Paleoenvironmental and Stratigraphic Implications of Taphonomic Processes: Case Studies from Recent and Pleistocene Shallow Marine Environments [unpub. Ph.D. thesis]: University of Arizona, Tucson, 440 p.

Oehmig, R., 1993, Entrainment of planktonic Foraminifera: Effect of bulk density: Sedimentology, v. 40, p. 869-877.

Ortlieb, L., 1981, Pleistocene interglacial high stands of sea level in the Gulf of California: Geological Society of America Abstracts with Programs, v. 13, p. 99.

Peebles, M.W., and Lewis, R.D., 1988, Differential infestation of shallow-water benthic Foraminifera by microboring organisms: Possible biases in preservation potential: PALAIOS, v. 3, p. 345-351.

Phleger, F.B., 1960, Ecology and Distribution of Recent Foraminifera: Baltimore, Johns Hopkins Press, 297 p.

Sanders, H.L., 1968, Marine benthic diversity: A comparative study: American Naturalist, v. 102, p. 243-282.

Sandusky, C.L., 1969, Sedimentology of Estero Marua, Sonora, Mexico [unpub. M.S. thesis]: University of Arizona, Tucson, 84 p.

Shroba, C.S., 1993, Taphonomic features of benthic Foraminifera in a temperate setting: Experimental and field observations on the role of abrasion, solution and microboring in the destruction of foraminiferal tests: PALAIOS, v. 8, p. 250-266.

Silva de Echols, C.M.H.M., 1993, Diatom infestation of recent crinoid ossicles in temperate waters, Friday Harbor Laboratories, Washington: Implications for biodegradation of skeletal carbonates: PALAIOS, v. 8, p. 278-288.

Sneed, E.D. and Folk, R.L., 1958, Pebbles in the lower Colorado River, Texas, a study in particle morphogenesis: Journal of Geology, v. 66, p. 114-150.

Stearley, R.F., and Ekdale, A.A., 1989, Modern marine bioerosion by macroinvertebrates, northern Gulf of California: PALAIOS, v. 4, p. 453-467.

Sumpter, L.T., 1987, Grain size and provenance of Bahia la Choya sediments: In Flessa, K.W., ed., Paleoecology and Taphonomy of Recent to Pleistocene Intertidal Deposits, Gulf of California, Paleontological Society Special Publication No. 2, p. 44-51.

Sundborg, A., 1956, The River Klarälven, a study of fluvial processes: Geografiska Annaler, v. 38, p. 125-316.

Tappan, H., and Loeblich, A.R., 1988, Foraminiferal evolution, diversification, and extinction: Journal of Paleontology, v. 62, p. 695-714.

Thomson, D.A., 1991-1992, Tide Calendars for the Northern Gulf of California: University of Arizona, Tucson, 12 p.

Wadell, H., 1932, Volume, shape, and roundness of rock particles: Journal of Geology, v. 40, p. 443-451.

Walker, D.A., Linton, A.E., and Schafer, C.T., 1974, Sudan Black B: A superior stain to rose bengal for distinguishing living from non-living Foraminifera: Journal of Foraminiferal Research, v. 4, p. 205-215.

Walton, W.R., 1955, Ecology of living benthonic Foraminifera, Todos Santos Bay, Baja California: Journal of Paleontology, v. 29, p. 952-1018.

Warg, J.B., 1973, An analysis of methods for calculating constant terminal-settling velocities of spheres in liquids: Mathematical Geology, v. 5, p. 59-72.

Zingg, T., 1935, Beiträge zur Schotteranalyse: Schweizerische Mineralogische und Petrographische Mitteilungen, v. 15, p. 39-140.

APPENDIX

APPENDIX

Raw Data for Settling and Movement-Threshold Velocities of Five Foraminiferal Species as well as Relevant Test Parameters

Specimen #	Species Code[a]	SetVel[b] (cm/sec)	T (F)[c] (cm/sec)	T (C)[d] (cm/sec)	Ds (mm)	Di (mm)	Dl (mm)	Weight (mg)	Volume (mm^3)	Porosity	DWAT[e] (mg/mm^3)	Ds/Di	Di/Dl	CSF	Dn (mm)	MPS	OS
100	Q1	2.3	2.0	6.0	0.24	0.32	0.50	0.022	0.020	0.59	1.69	0.75	0.64	0.60	0.34	0.71	0.67
101	Q1	1.8	1.0	12.0	0.24	0.32	0.46	0.018	0.019	0.63	1.63	0.75	0.70	0.63	0.33	0.73	0.71
102	Q1	1.8	1.0	6.0	0.22	0.30	0.46	0.016	0.016	0.64	1.62	0.73	0.65	0.59	0.31	0.71	0.68
103	Q1	2.1	5.0	21.0	0.24	0.34	0.48	0.019	0.021	0.66	1.59	0.71	0.71	0.59	0.34	0.71	0.71
104	Q1	1.5			0.20	0.26	0.42	0.011	0.011	0.65	1.60	0.77	0.62	0.61	0.28	0.72	0.67
105	Q1	1.5			0.21	0.26	0.39	0.012	0.011	0.61	1.67	0.81	0.67	0.66	0.28	0.76	0.71
106	Q1	2.0			0.23	0.34	0.58	0.020	0.024	0.69	1.53	0.68	0.59	0.52	0.36	0.64	0.61
107	Q1	1.4	1.0	18.0	0.20	0.23	0.44	0.008	0.011	0.71	1.50	0.87	0.52	0.63	0.27	0.73	0.62
108	Q1	1.9			0.24	0.34	0.48	0.017	0.021	0.69	1.53	0.71	0.71	0.59	0.34	0.71	0.71
109	Q1	2.3	7.0	1.0	0.29	0.36	0.54	0.024	0.030	0.70	1.51	0.81	0.67	0.66	0.38	0.76	0.71
110	Q1	1.9			0.28	0.42	0.70	0.023	0.043	0.80	1.33	0.67	0.60	0.52	0.44	0.64	0.62
111	Q1	1.6	3.0	12.0	0.20	0.26	0.44	0.010	0.012	0.68	1.54	0.77	0.59	0.59	0.28	0.70	0.65
112	Q1	2.1	1.0	12.0	0.28	0.35	0.36	0.026	0.019	0.49	1.88	0.80	0.97	0.79	0.33	0.85	0.91
113	Q1	2.1	1.0	7.0	0.26	0.36	0.57	0.026	0.028	0.65	1.59	0.72	0.63	0.57	0.38	0.69	0.66
115	Q1	1.6			0.22	0.30	0.50	0.013	0.017	0.73	1.46	0.73	0.60	0.57	0.32	0.69	0.64
116	Q1	1.5			0.17	0.23	0.42	0.008	0.009	0.64	1.61	0.74	0.55	0.55	0.25	0.67	0.61
117	Q1	2.2	3.0	7.0	0.28	0.36	0.58	0.023	0.031	0.72	1.48	0.78	0.62	0.61	0.39	0.72	0.67
118	Q1	1.8	4.0	3.0	0.26	0.35	0.54	0.022	0.026	0.68	1.54	0.74	0.65	0.60	0.37	0.71	0.68
119	Q1	1.8	2.0	16.0	0.20	0.28	0.48	0.015	0.014	0.61	1.66	0.71	0.58	0.55	0.30	0.67	0.62
120	Q1	1.6	1.0	5.0	0.28	0.37	0.58	0.016	0.032	0.81	1.31	0.76	0.64	0.60	0.39	0.71	0.68
121	B1	1.9			0.28	0.44	0.50	0.015	0.032	0.83	1.29	0.64	0.88	0.60	0.39	0.71	0.79
122	B1	2.2			0.22	0.41	0.50	0.020	0.024	0.69	1.52	0.54	0.82	0.49	0.36	0.62	0.71
123	B1	2.5	7.0	11.0	0.30	0.46	0.54	0.023	0.039	0.78	1.37	0.65	0.85	0.60	0.42	0.71	0.78
124	B1	1.5			0.25	0.36	0.40	0.010	0.019	0.81	1.32	0.69	0.90	0.66	0.33	0.76	0.83
125	B1	1.5			0.23	0.35	0.40	0.009	0.017	0.81	1.32	0.66	0.88	0.61	0.32	0.72	0.80
126	B1	1.5			0.23	0.36	0.44	0.009	0.019	0.82	1.30	0.64	0.82	0.58	0.33	0.69	0.75
127	B1	1.6			0.23	0.34	0.42	0.009	0.017	0.81	1.33	0.68	0.81	0.61	0.32	0.72	0.76
128	B1	1.8			0.28	0.41	0.44	0.013	0.026	0.82	1.30	0.68	0.93	0.66	0.37	0.76	0.84
129	B1	1.5			0.24	0.38	0.42	0.009	0.020	0.84	1.27	0.63	0.90	0.60	0.34	0.71	0.80
130	B1	1.8			0.30	0.42	0.47	0.012	0.031	0.86	1.24	0.71	0.89	0.68	0.39	0.77	0.83
131	B1	1.3			0.22	0.30	0.35	0.006	0.012	0.83	1.29	0.73	0.86	0.68	0.28	0.77	0.81
132	B1	1.8			0.26	0.38	0.44	0.011	0.023	0.82	1.30	0.68	0.86	0.64	0.35	0.74	0.80
133	B1	2.6	1.0	6.0	0.26	0.38	0.44	0.028	0.023	0.55	1.77	0.68	0.86	0.64	0.35	0.74	0.80
134	B1	1.9	1.0	13.0	0.23	0.32	0.40	0.018	0.015	0.56	1.75	0.72	0.80	0.64	0.31	0.74	0.77
135	B1	2.1	1.0	8.0	0.26	0.38	0.41	0.019	0.021	0.67	1.56	0.68	0.93	0.66	0.34	0.76	0.84
141	B1	2.2	3.0	7.0	0.24	0.31	0.38	0.017	0.015	0.57	1.73	0.77	0.82	0.70	0.30	0.79	0.80
142	B1	1.5	4.0	11.0	0.28	0.35	0.42	0.017	0.022	0.71	1.50	0.80	0.83	0.73	0.35	0.81	0.82
143	B1	1.9	4.0	19.0	0.24	0.34	0.40	0.016	0.017	0.65	1.60	0.71	0.85	0.65	0.32	0.75	0.80
144	B1	2.0	1.0	16.0	0.28	0.38	0.44	0.014	0.025	0.79	1.36	0.74	0.86	0.68	0.36	0.78	0.82
145	B1	1.9	1.0	18.0	0.26	0.41	0.50	0.015	0.028	0.80	1.34	0.63	0.82	0.57	0.38	0.69	0.75
146	B1	2.1	1.0	17.0	0.32	0.41	0.49	0.019	0.034	0.80	1.35	0.78	0.84	0.71	0.40	0.80	0.82
158	E1	1.4	1.0		0.20	0.32	0.36	0.009	0.012	0.73	1.45	0.63	0.89	0.59	0.28	0.70	0.79
159	E1	2.5	1.0	8.0	0.26	0.38	0.44	0.030	0.023	0.51	1.83	0.68	0.86	0.64	0.35	0.74	0.80
160	E1	2.2	8.0	12.0	0.24	0.37	0.46	0.021	0.021	0.65	1.60	0.65	0.80	0.58	0.34	0.70	0.75
161	E1	1.9			0.20	0.36	0.40	0.015	0.015	0.64	1.61	0.56	0.90	0.53	0.31	0.65	0.77
162	E1	1.4			0.19	0.32	0.38	0.008	0.012	0.76	1.40	0.59	0.84	0.54	0.28	0.67	0.75
163	E1	1.5			0.22	0.34	0.40	0.010	0.016	0.76	1.40	0.65	0.85	0.60	0.31	0.71	0.78
164	E1	1.8			0.22	0.28	0.32	0.010	0.010	0.63	1.63	0.79	0.88	0.74	0.27	0.81	0.84
165	E1	1.3			0.18	0.30	0.36	0.008	0.010	0.72	1.48	0.60	0.83	0.55	0.27	0.67	0.75
166	E1	2.4	8.0	7.0	0.24	0.46	0.54	0.030	0.031	0.65	1.60	0.52	0.85	0.48	0.39	0.61	0.72
167	E1	1.6			0.20	0.32	0.40	0.013	0.013	0.64	1.61	0.63	0.80	0.56	0.29	0.68	0.74
168	E1	2.3	15.0	9.0	0.22	0.36	0.40	0.020	0.017	0.56	1.75	0.61	0.90	0.95	0.32	0.70	0.79
169	E1	1.6			0.18	0.32	0.38	0.012	0.012	0.63	1.63	0.56	0.84	0.52	0.28	0.64	0.74
170	E1	1.6			0.18	0.26	0.32	0.009	0.008	0.58	1.71	0.69	0.81	0.62	0.25	0.73	0.77
171	E1	1.8			0.24	0.36	0.44	0.015	0.020	0.72	1.48	0.67	0.82	0.60	0.34	0.71	0.76
172	E1	1.3			0.18	0.28	0.32	0.007	0.008	0.70	1.51	0.64	0.88	0.60	0.25	0.71	0.79
173	E1	2.3			0.24	0.38	0.44	0.023	0.021	0.60	1.68	0.63	0.86	0.59	0.34	0.70	0.78
174	E1	1.9			0.22	0.32	0.40	0.016	0.015	0.61	1.67	0.69	0.80	0.61	0.30	0.72	0.76
175	E1	2.1	7.0	7.0	0.23	0.38	0.46	0.019	0.021	0.66	1.58	0.61	0.83	0.55	0.34	0.67	0.74

APPENDIX-Continued.

Specimen #	Species Code[a]	SetVel[b] (cm/sec)	T (F)[c] (cm/sec)	T (C)[d] (cm/sec)	Ds (mm)	Di (mm)	Dl (mm)	Weight (mg)	Volume (mm^3)	Porosity	DWAT[e] (mg/mm^3)	Ds/Di	Di/Dl	CSF	Dn (mm)	MPS	OS
176	E1	1.2			0.16	0.30	0.34	0.006	0.009	0.76	1.41	0.53	0.88	0.50	0.25	0.63	0.75
178	E2	1.4	1.0	2.0	0.17	0.30	0.38	0.007	0.010	0.75	1.42	0.57	0.79	0.50	0.27	0.63	0.71
179	E2	1.4	11.0	18.0	0.17	0.30	0.36	0.011	0.010	0.59	1.69	0.57	0.83	0.52	0.26	0.64	0.73
180	E2	1.4			0.21	0.38	0.44	0.010	0.018	0.80	1.35	0.55	0.86	0.51	0.33	0.64	0.74
181	E2	1.2			0.20	0.35	0.46	0.008	0.017	0.82	1.31	0.57	0.76	0.50	0.32	0.63	0.69
182	E2	1.3			0.16	0.30	0.34	0.008	0.009	0.67	1.56	0.53	0.88	0.50	0.25	0.63	0.75
183	E2	1.3			0.14	0.26	0.33	0.006	0.006	0.64	1.62	0.54	0.79	0.48	0.23	0.61	0.69
184	E2	0.8			0.14	0.28	0.34	0.004	0.007	0.78	1.38	0.50	0.82	0.45	0.24	0.59	0.70
185	E2	1.3			0.21	0.42	0.51	0.011	0.024	0.83	1.29	0.50	0.82	0.45	0.36	0.59	0.70
186	E2	1.2			0.17	0.32	0.40	0.006	0.011	0.82	1.30	0.53	0.80	0.48	0.28	0.61	0.70
187	E2	0.9			0.14	0.25	0.30	0.005	0.006	0.67	1.56	0.56	0.83	0.51	0.22	0.64	0.73
188	E2	1.4	1.0	22.0	0.24	0.42	0.50	0.013	0.026	0.81	1.32	0.57	0.84	0.52	0.37	0.65	0.74
189	E2	1.5	3.0	13.0	0.19	0.38	0.44	0.011	0.017	0.76	1.41	0.50	0.86	0.46	0.32	0.60	0.72
190	E2	1.5	9.0	18.0	0.20	0.38	0.44	0.010	0.018	0.78	1.37	0.53	0.86	0.49	0.32	0.62	0.73
191	E2	1.6	13.0	8.0	0.18	0.32	0.38	0.011	0.012	0.64	1.62	0.56	0.84	0.52	0.28	0.64	0.74
192	E2	1.1			0.14	0.22	0.27	0.006	0.004	0.51	1.83	0.64	0.81	0.57	0.20	0.69	0.75
193	E2	1.5			0.20	0.36	0.42	0.015	0.016	0.66	1.58	0.56	0.86	0.51	0.31	0.64	0.74
194	E2	1.1			0.18	0.30	0.36	0.011	0.010	0.60	1.68	0.60	0.83	0.55	0.27	0.67	0.75
195	E2	1.4	5.0	18.0	0.20	0.29	0.35	0.009	0.011	0.70	1.50	0.69	0.83	0.63	0.27	0.73	0.78
196	E3	3.9	1.0	7.0	0.38	0.65	0.72	0.091	0.093	0.64	1.62	0.58	0.90	0.56	0.56	0.68	0.78
197	E3	3.2			0.34	0.64	0.70	0.070	0.080	0.68	1.55	0.53	0.91	0.51	0.53	0.64	0.76
198	E3	3.9			0.40	0.64	0.76	0.091	0.102	0.67	1.56	0.63	0.84	0.57	0.58	0.69	0.76
199	E3	4.5			0.41	0.68	0.80	0.119	0.117	0.62	1.64	0.60	0.85	0.56	0.61	0.68	0.76
200	E3	3.4			0.32	0.56	0.64	0.065	0.060	0.60	1.68	0.57	0.88	0.53	0.49	0.66	0.76
201	E3	2.8	5.0	13.0	0.25	0.42	0.48	0.031	0.026	0.57	1.74	0.60	0.88	0.56	0.37	0.68	0.77
202	E3	2.1			0.23	0.43	0.48	0.021	0.025	0.69	1.52	0.53	0.90	0.51	0.36	0.64	0.75
203	E3	2.9			0.31	0.52	0.59	0.046	0.050	0.66	1.57	0.60	0.88	0.56	0.46	0.68	0.77
204	E3	2.7			0.32	0.54	0.63	0.044	0.057	0.72	1.48	0.59	0.86	0.55	0.48	0.67	0.76
205	E3	3.2	1.0	12.0	0.31	0.52	0.60	0.052	0.051	0.62	1.64	0.60	0.87	0.56	0.46	0.68	0.77
206	E3	2.6	1.0	13.0	0.28	0.46	0.52	0.036	0.035	0.62	1.65	0.61	0.88	0.57	0.41	0.69	0.78
207	E3	2.2	7.0	17.0	0.25	0.38	0.45	0.023	0.022	0.62	1.65	0.66	0.84	0.60	0.35	0.72	0.78
208	E3	3.2	4.0	7.0	0.32	0.51	0.62	0.058	0.053	0.59	1.69	0.63	0.82	0.57	0.47	0.69	0.75
209	E3	2.1	5.0	11.0	0.25	0.46	0.50	0.031	0.030	0.62	1.65	0.54	0.92	0.52	0.39	0.65	0.77
210	E3	3.1	7.0	4.0	0.29	0.50	0.58	0.055	0.044	0.54	1.79	0.58	0.86	0.54	0.44	0.66	0.76

[a] Q1=*Quinqueloculina seminulum*; B1=*Buccella mansfieldi*; E1=*Elphidium* cf. *E. gunteri*; E2=*Elphidium articulatum* var. *E. rugulosum*; E3=*Elphidium* cf. *E. crispum*.
[b] SetVel refers to settling velocity.
[c] T (F) refers to threshold velocity with a fixed fine-sand platform.
[d] T (C) refers to threshold velocity with a fixed coarse-sand platform.
[e] DWAT refers to effective density in water.